Widespread Origin of the Primate Mesofrontal Dopamine System

S. Mark Williams[1] and Patricia S. Goldman-Rakic

Section of Neurobiology, C303 SHM, Yale University School of Medicine, PO Box 208001, New Haven, CT 06510, USA

[1]Current address: Department of Neurobiology, Duke University Medical Center, PO Box 3209, Durham, NC 27710, USA, markw@neuro.duke.edu

The dopaminergic innervation of the frontal cortex, commonly implicated in psychiatric and neurological disorders, has traditionally been associated with a circumscribed midline group of ventral tegmental area (VTA) neurons. We have employed a combination of retrograde tracing, using fluorescent dyes, and tyrosine hydroxylase (TH) immunohistochemistry to amplify knowledge of frontal cortex-projecting dopamine (DA) neurons in non-human primates. Injections of retrograde fluorochromes were made in areas 46, 8B/6M, 12, 4, 24, and the prelimbic (PL) and infralimbic areas (IL) of the rhesus monkey. The mesencephalic distribution of neurons exhibiting both retrograde labeling and TH immunoreactivity or retrograde labeling alone was examined from the level of the mammillary bodies to the locus coeruleus. DA afferents innervating the macaque frontal cortex as a whole originate from an unexpectedly widespread continuum of neurons distributed in the dorsal aspects of all three of the mesencephalic DA cell groups [A9, A10 and A8; generally corresponding to the DA cells of the substantia nigra (SN), VTA, and the retrorubral area (RRA) respectively]. A large number of these retrogradely labeled neurons are non-dopaminergic. The dorsal frontal cortex (areas 46, 8B/6M and 4) receive DA projections primarily from the full medial-lateral extent of A9 cells dorsal to the SN pars compacta (i.e. A9 dorsalis), the RRA and to a lesser extent from the A10 parabrachial pigmented nucleus (PBPG) and linear nuclei, the latter of which have been associated with the mesocortical DA system. In contrast, the ventromedial PL and IL exhibit a significantly more robust input from the PBPG and midline linear VTA nuclei than from the lateral groups. The anterior cingulate cortex (area 24) is innervated by a group of DA neurons primarily located between these laterally and medially concentrated populations. These findings demonstrate a degree of compartmentalization of the mesofrontal DA system in primates, and suggest that this projection should no longer be viewed as a unitary midline system.

Introduction

Recent models of cognitive dysfunction in schizophrenia and of the action of antipsychotic (AP) drugs, particularly the atypical APs, have invoked a hodological scheme which emphasizes the functional significance of the mesocortical dopamine (DA) system. This is due in large part to the repeated association of the DA innervation of the dorsolateral prefrontal cortex (dlPFC) with cognitive operations, such as spatial working memory processes (Brozoski *et al.*, 1979; Sawaguchi and Goldman-Rakic, 1991; Luciana *et al.*, 1992; Williams and Goldman-Rakic, 1995; Kishka *et al.*, 1996; Murphy *et al.*, 1996a,b; Luciana and Collins, 1997) and the increasing demonstration of the pathophysiology of this region in schizophrenia (e.g. Benes *et al.*, 1991; Pettegrew *et al.*, 1991; Akbarian *et al.*, 1993; Glantz and Lewis, 1993; Selemon *et al.*, 1995). As schizophrenic patients have demonstrated significant deficits on working memory tasks (Park and Holzman, 1992), the DA innervation of the dlPFC represents a promising target for the design of novel drugs which combat deficit symptoms associated with this and other psychiatric disorders.

Evidence continues to accumulate demonstrating that the mesocortical DA projection is functionally distinct from the neighboring mesostriatal and mesolimbic pathways. However, the specific morphological organization and biochemical characteristics underlying the unique physiology of these systems are only beginning to be elucidated (Deutch *et al.*, 1991, 1993). An initial step in this process is to establish a detailed understanding of the anatomical organization of the mesocortical system at both the terminal field and brainstem levels. Clearly, knowledge regarding the organization of the mesocortical DA system in primates is limited, as compared to the rodent, particularly at the level of the mesencephalon. This is especially significant because of the elaboration and differentiation of the cerebral cortex in primates and the substantial evidence of species differences in the organization of the cortical DA innervation (reviewed in Berger *et al.*, 1991). Whereas DA afferents are found in high densities primarily in the prefrontal and cingulate areas of the rodent neocortex, DA axons heavily innervate most regions of the frontal cortex, as well as many temporal and parietal areas, of macaques (Levitt *et al.*, 1984; Lewis *et al.*, 1987; Berger *et al.*, 1986, 1988; Gaspar *et al.*, 1989; Williams and Goldman-Rakic, 1993). DA afferents also demonstrate an expanded laminar innervation in all of these regions. Although there have been a few studies of the brainstem origin of the mesofrontal DA system in the primate (Porrino and Goldman-Rakic, 1982; Oeth and Lewis, 1992; Gaspar *et al.*, 1992, 1993), none have examined specifically the topography and origin of histochemically identified DA neurons innervating the frontal cortex of the macaque, the primate species in which many morphological and functional aspects of the cortical DA system have been examined (Lewis *et al.*, 1987, 1988; Berger *et al.*, 1988; Smiley and Goldman-Rakic, 1993; Williams and Goldman-Rakic, 1993, 1995; Smiley *et al.*, 1994; Sesack *et al.*, 1995). Furthermore, the mesencephalic origin of the medial prefrontal DA innervation has not been studied to date in any primate species. Given the particularly salient functional properties of this projection in rodents, it is of considerable interest to examine the potential homologue of this afferent system in primates.

In the present study, we have injected selected dorsolateral and medial frontal cortical areas of the macaque with fluorescent retrograde tracers and have identified the presence of dopamine in retrogradely labeled (RL) neurons immunohistochemically using an antibody directed against tyrosine hydroxylase (TH). The areas injected include the principal sulcus (area 46), area 8B, the supplementary motor cortex (area 6M), the dorsomedial primary motor cortex (area 4), area 24, and the prelimbic (PL) and infralimbic (IL) areas. In order to elucidate the organizational principles of the mesofrontal DA system at the brainstem

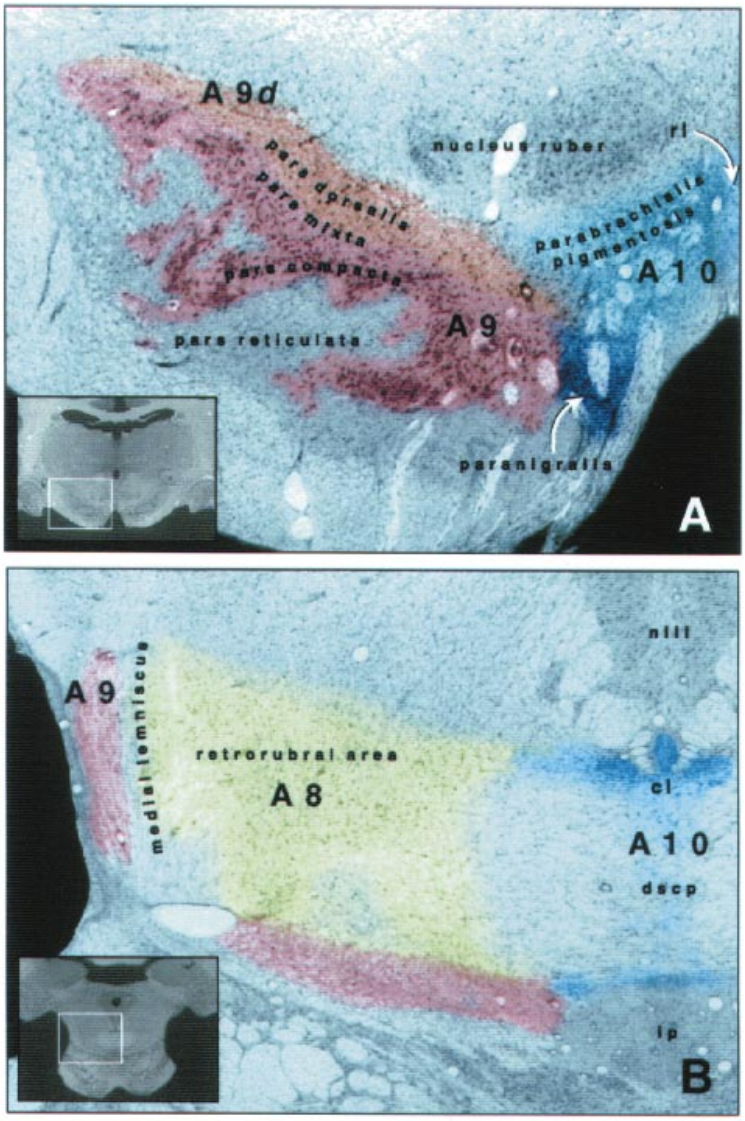

Figure 1. Dopaminergic cell groups of the ventral mesencephalon (VM). (*A*) Cresyl violet-stained section of the rostral VM at the level of the oculomotor nerve rootlets, colorized to indicate the approximate locations of A10 (blue hues) and A9 (red hues) dopamine neurons. The A10 DA cells are distributed in five nuclei of the VMT: the dorsally situated PBPG, the more ventral PN, and the three midline nuclei, RL, IF (located ventral to RL) and CL. The A9 neurons are distributed in the substantia nigra pars compacta and a region of more loosely aggregated cells situated dorsal to the SNpc and lateral to the PBPG, referred to in the present study as A9*d*. This region includes the pars mixta of Francois *et al.* (1985) and the pars dorsalis of Poirier *et al.* (1983). *Inset*: low-power view of midbrain section illustrating the region enlarged in (*A*). (*B*) Cresyl violet-stained section of the caudal VM at the level of the decussation of superior cerebellar peduncle. A8 DA neurons (yellow) are distributed in the mesencephalic reticular formation lateral to the DSCP and medial to the medial lemniscus (some authors consider the DA neurons lateral to the medial lemniscus, lateral A8 cells; see Deutch *et al.*, 1986). As the A8 region roughly corresponds to the location of the retrorubral nucleus in carnivores, this area is often referred to as the retrorubral area. At this level, some A9 neurons are also present ventral and lateral to A8 cells. *Inset*: low-power view of midbrain section illustrating the region enlarged in (*B*). As midbrain DA cells are distributed in a continuum, the precise boundaries between the A8, A9 and A10 groups, as well as between the component nuclei of these groups are for the most part indiscernible. This is especially the case for the borders between the SNpc, the PBPG and the loosely organized DA cells of the midbrain reticular formation. It is in these transitional zones that the vast majority of mesofrontal DA neurons reside. See text for abbreviations.

level, we sought to determine the distribution of frontal cortex-projecting DA neurons as a whole, to examine whether they are localized to a specific mesencephalic nucleus or DA cell group (e.g. A10), whether these projections are organized topographically and/or exhibit areal or regional differences, and finally, whether all mesencephalic cortically projecting neurons contain dopamine.

Materials and Methods

Surgical Methods

Thirteen young adult (2–3 years old) rhesus monkeys (*Macaca mulatta*) were used in the present study. Eleven of these received injections confined to one cortical region. In two of the 13 monkeys, two retrograde fluorochromes were injected into distinct regions to provide the possibility of assessing the degree of colateralizaton of mesofrontal DA afferents. Animals were anesthetized with sodium pentobarbital and the frontal cortical area of interest was exposed with a craniotomy and reflection of the dura mater. Sulcal landmarks and magnetic resonance imaging (MRI) were used to determine the location of frontal cortical areas and the placement of fluorochrome injections.

To produce adequate labeling of cortically projecting midbrain cells, relatively large regions, often involving more than one cytoarchitectonic area, were injected with fast blue, diamidino yellow and fluororuby. Surgical exposure of the dorsolateral surface of the frontal cortex afforded

the opportunity to place numerous small injections of tracer into the cortical gray matter. After limited success of labeling mesencephalic neurons following 'typical' pressure injections of the retrograde fluorochrome (~100–300 nl per tract, ~3–4 tracts in a given cytoarchitectonic area), we increased the number of penetrations in the area while maintaining approximately the same volume of tracer per penetration. Thus, for a given area of frontal cortex, numerous (30–80) penetrations (using Hamilton 1 and 5 µl syringes) were made, separated by ~1–2 mm, of ~100–300 nl for a total volume of 8–16 µl (see Figs 2–7). Although some tissue damage of the injection site was produced with this method, we nevertheless observed significantly better transport to the brainstem than with more limited injections. This technique was used for the dorsolateral and dorsomedial areas (areas 46, 8B, 6M and 4); for cortical areas on the midline, e.g. area 24 and PL, in which the cortical surface is not exposed, we were not able to inject in this manner. For these medial frontal cortical injections we utilized MRI to guide the stereotaxic placement of the fluorochrome-filled microsyringes (Fig. 3). Two or three penetrations, separated by a millimeter or two in the rostrocaudal dimension, were made for each area. Retrograde tracer was deposited at various dorsal-ventral points in the tract and thus a relatively large injection (approximate total volume 8 µl) of fluorochrome was made.

We had only moderate success in labeling ventral mesencephalic cells using fluorescent retrograde tracers other than fast blue, e.g. diamidino yellow, fluorogold, fluororuby and green latex beads, and thus employed fast blue in the majority of cases. Interestingly, in most cases, these other fluorochromes did yield robust RL neurons in the thalamus and distal cortical areas. Additionally, we successfully retrogradely labeled ventral mesencephalon neurons with fluororuby and diamidino yellow following injections in the dorsal and ventral striatum (S.M. Williams and P.S. Goldman-Rakic, in preparation).

Histological Methods

Following survival times of 10–14 days, animals were deeply anesthetized with barbiturate (pentobarbital 100 mg/kg, administered i.v.) and transcardially perfused, first with ~500 ml of heparinized 0.1 M phosphate-buffered saline (PBS; pH 7.4), followed by ~2–2.5 l of ice-cold fixative containing 4% paraformaldehyde in 0.1 M PB (pH 7.4). After removal from the cranium, the brains were cut into coronal blocks ~1 cm thick and post-fixed for 1 h in the fixative solution. Blocks then were placed overnight in a 0.1 M PB solution (pH 7.4) containing 10% sucrose, followed by 12 h incubation in 20% sucrose (4°C). Following this cryoprotection regimen, the tissue blocks were frozen rapidly in isopentane cooled by dry ice, and prior to processing stored at –70°C for immunocytochemistry.

Serial cryostat sections (40 µm) were placed in wells containing cold 0.05 M PB and processed for tyrosine hydroxylase (TH) immunoreactivity [immunofluorescence or diaminobenzidine (DAB)] and calbindin D_{28k} immunoreactivity. Adjacent sections were mounted on gelatinized slides, air dried and stained for Nissl substance with cresyl violet (or thionin) or stained for myelin with the Gallyas (1979) silver technique. For TH immunohistochemistry, sections were washed (3 × 10 min) in 0.05 M PBS (pH 7.4). Sections were then placed in blocking serum (PB containing 1% bovine serum albumin and 5% normal goat serum) prior to incubation in primary antisera. The primary antibodies, a rabbit polyclonal against TH (*Pel Freeze*) was used at a dilution of 1:1000 (diluted in blocking solution) and a monoclonal against calbindin was used at a dilution of 1:2000. Sections were incubated in the primary antibody for 48 h on a rotating device at 4°C. Following this incubation, sections were washed thoroughly in PB, and then incubated in a 1:200 dilution of the secondary antiserum (biotinylated anti-rabbit IgG) for 1.5 h at room temperature. After another series of washes in PB (pH 8.2) (3 × 10 min) sections were incubated in either avidin–FITC or avidin–rhodamine (Vector Labs) at a dilution of 1:50 in PB (pH 8.2) for ~6 h at room temperature.

For peroxidase DAB-stained material, the protocol was identical, except that following the incubation in the secondary antibody, sections were placed in ABC reagent (Vector Labs) (dilution of 1:125 in PB) for 2 h at room temperature. The peroxidase was revealed by incubating the tissue sections in a solution of 0.07% 3,3′-diaminobenzidine and 0.002% H_2O_2 (in PB) for 5–10 min. A negative control in which normal serum was substituted for the primary anti-TH antibody was employed as a check for the specificity of the immunolabeling. No specific immunostaining was observed under these conditions.

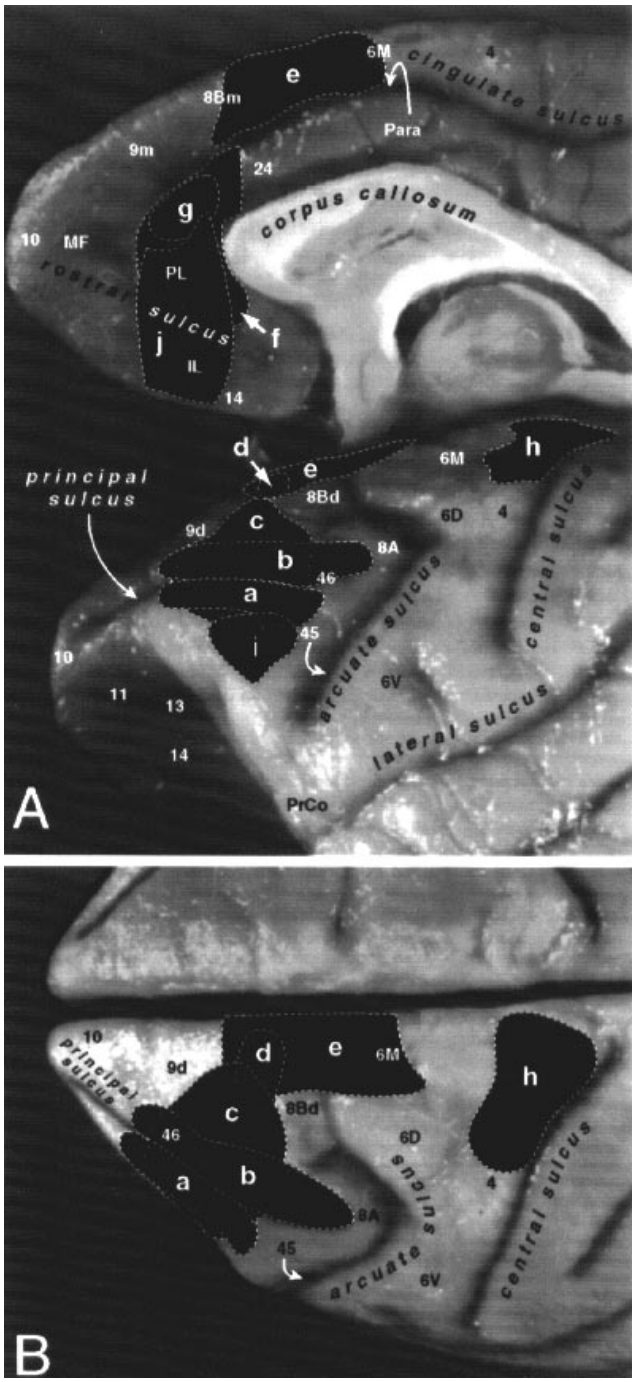

Figure 2. Midsagittal, lateral (*A*) and dorsal (*B*) views of the macaque brain illustrating the locations of the fast blue (a–h; j) and diamidino yellow (i) injection sites in the nine cases reported in the present study. See Figure 5*B* for (b) and (*i*); Figure 5*A* for (c); Figure 7*A* for (e); Figure 6*A* for (f); Figure 6*B* for (g); Figure 4 for (h); and Figure 7*B* for (j). Cytoarchitectonic areas of the macaque frontal lobe after Preuss and Goldman-Rakic (1991).

Following immunostaining, immunofluorescent sections were mounted onto gelatinized slides, air dried and stored at 4°C, until analyzed. Just prior to analysis, immunofluorescent sections were briefly dehydrated and quickly coverslipped using DPX. Immunostained sections

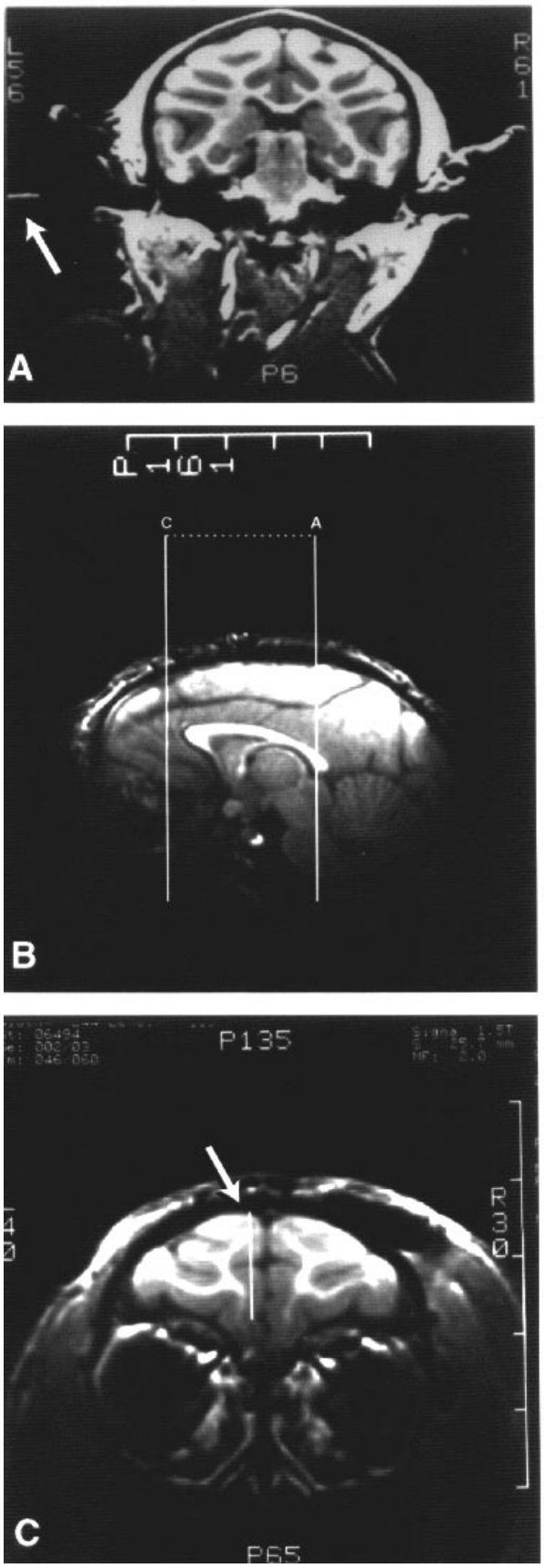

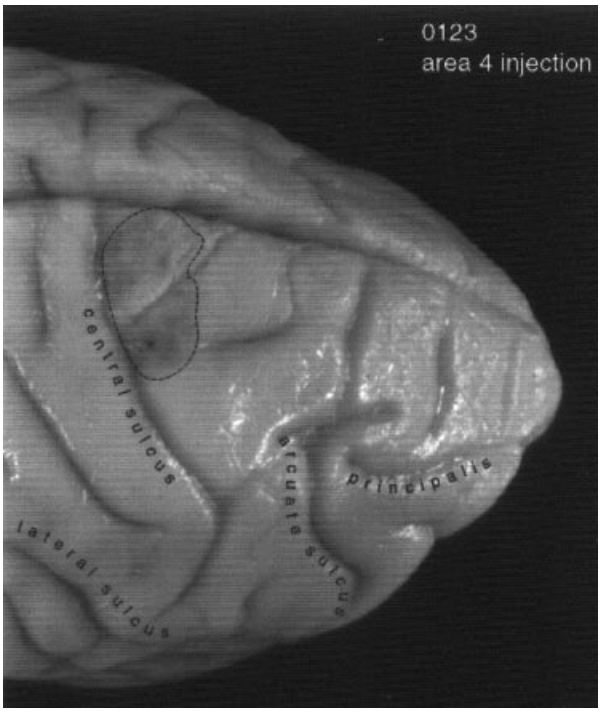

Figure 4. Photograph of the right macaque frontal lobe from case 0102 illustrating the injection site (dotted line) in the dorsomedial primary motor cortex (area 4). Numerous small injections of fast blue were made in this region.

Figure 3. Images of the macaque brain derived from magnetic resonance imaging, illustrating the method of deriving stereotaxic coordinates for the fast blue injections in the medial frontal cortex (area 24, prelimbic and infralimbic areas). (*A*) Caudal coronal image of the macaque brain in which the left ear bar (arrow) is observed. Mineral oil-filled ear bars allowed for the precise determination of the stereotaxic ear bar 0 (EB0), the reference point for determining the anterior-posterior coordinates of the injections. (*B*) Midsagittal image illustrating the locations of the coronal images in (*A*) and (*C*). (*C*) Coronal section of the macaque prefrontal cortex illustrating the trajectory of the microsyringe penetration into the prelimbic area (arrow). The center of the superior sagittal sinus was used as a medio-lateral zero point (ML0) from which the appropriate lateral deviation was calculated from the MRI films. Dorso-ventral coordinates were determined using the surface of the dura as a reference.

for TH (DAB) and calbindin D_{28k} also were counterstained with thionin and used in the determination of mesencephalic DA cell groups.

Delineation of Mesencephalic Dopaminergic Cell Groups

Sections stained for Nissl substance and myelin, as well as TH and calbindin D-28k immunoreactivity, were used to determine the locations of the ventral mesencephalic dopamine cell groups in the primate brainstem (Fig. 1). The virtual absence of noradrenergic neurons in the midbrain renders TH a specific marker for DAergic cells in the mesencephalon (see Arsenault *et al.*, 1988; Deutch *et al.*, 1988; Gaspar *et al.*, 1992).

Although dopamine neurons are distributed in a widespread, continuous network throughout the mesencephalon, Dahlstrom and Fuxe (1964) introduced a tripartite division of the DA midbrain cells, designated A8, A9 and A10, based on DA cellular morphology and general topography, which serves as the basic organizational framework for the present analysis. These three loci are often used broadly and interchangeably with three cytoarchitectonically defined regions of the ventral mesencephalon: (i) the ventromedial mesencephalic tegmentum (VMT) (A10 [referred to as the ventral tegmental area (VTA) in some nomenclatures]); (ii) the pars compacta and dorsal contiguous zones of the substantia nigra (A9); and (iii) the retrorubral area (RRA) (or field)

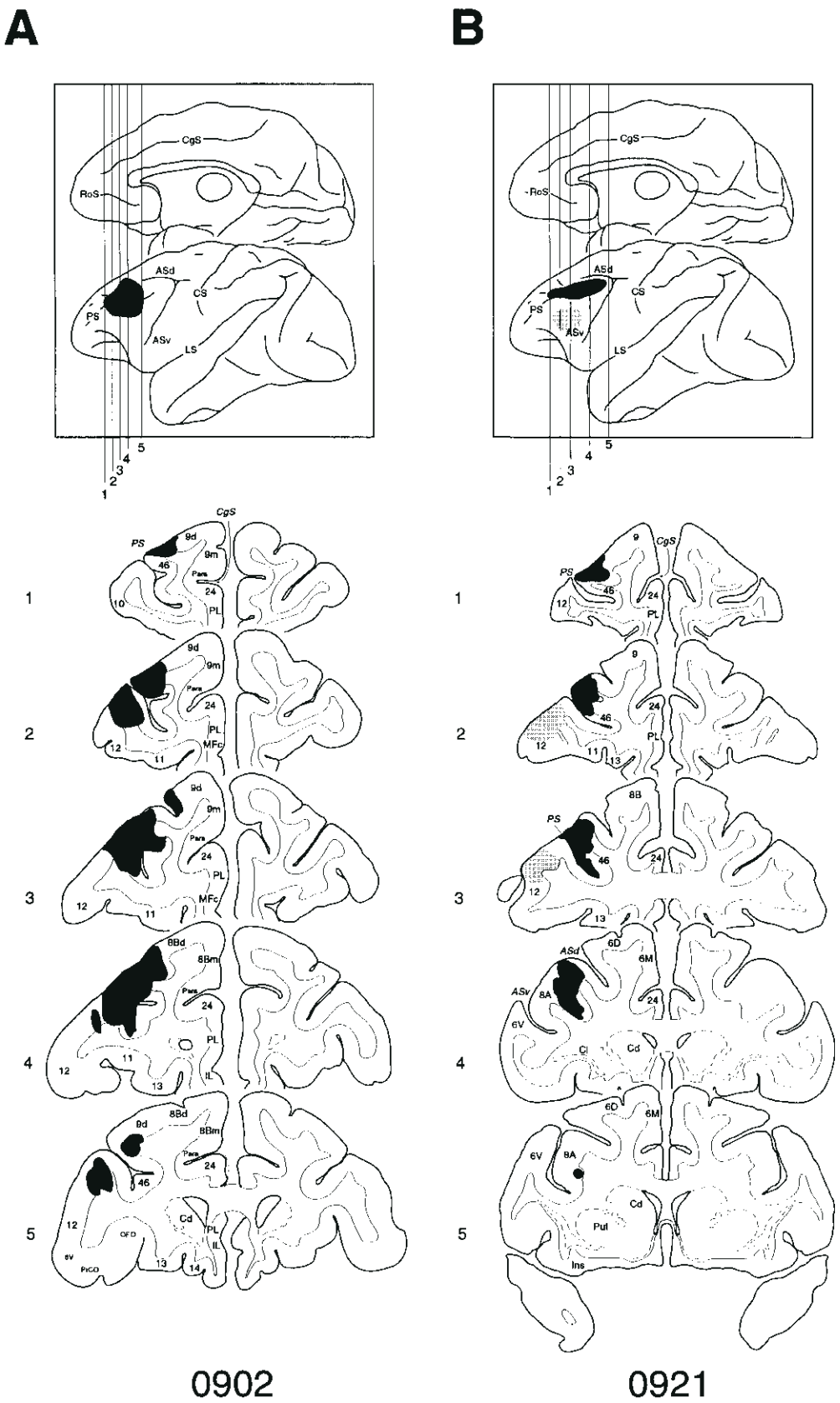

Figure 5. (*A*) Camera lucida drawings of coronal sections of the macaque frontal lobe from case 0902 illustrating a fast blue injection in the region of the principal sulcus. The lateral portions of areas 9d and 8Bd were also included in this site. (*B*) Camera lucida drawings of coronal sections of the macaque frontal lobe from case 0921 illustrating a fast blue injection site in the region of the principal sulcus (black) and a diamidino yellow injection in area 12vl (gray). Fast blue was primarily localized in the dorsal bank and rim of the PS, but included rostral area 8A. *Top*: Medial and lateral schematic views of the macaque cerebral cortex illustrating the anterior–posterior location of the coronal sections below. See text for details.

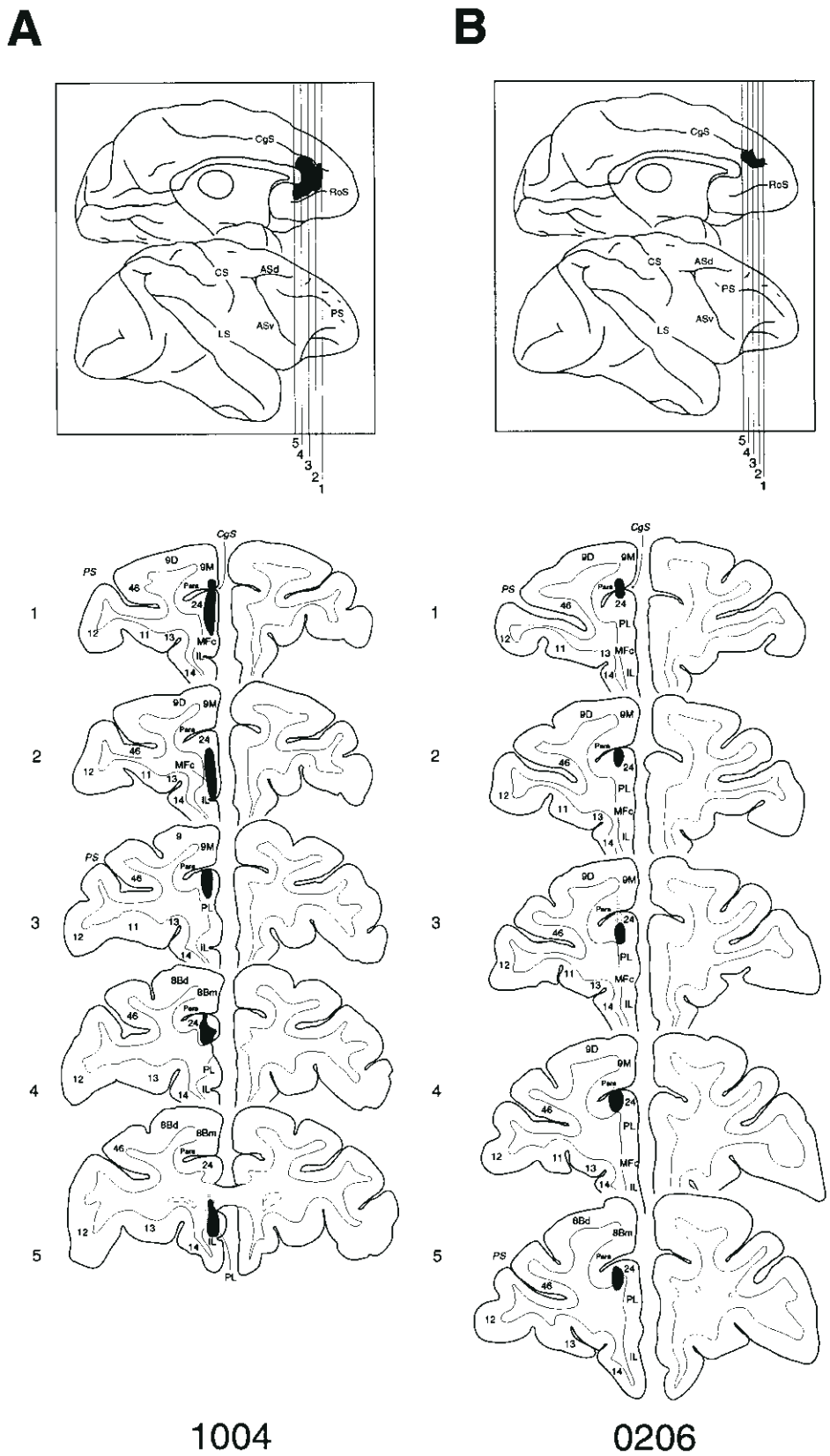

Figure 6. (*A*) Camera lucida drawings of coronal sections of the macaque frontal lobe from case 1004 illustrating a fast blue injection site in the medial frontal cortex. The injection is centered in the prelimbic area, but also includes part of the overlying paralimbic cortex, area 24 and the dorsal aspect of the infralimbic area. (*B*) Camera lucida drawings of coronal sections of the macaque frontal lobe from case 0206 illustrating a fast blue injection site in the medial frontal cortex. The injection is centered in area 24, but also includes part of the overlying paralimbic cortex. *Inset*: Medial and lateral schematic views of the macaque cerebral cortex illustrating the anterior–posterior location of the coronal sections below. See text for details.

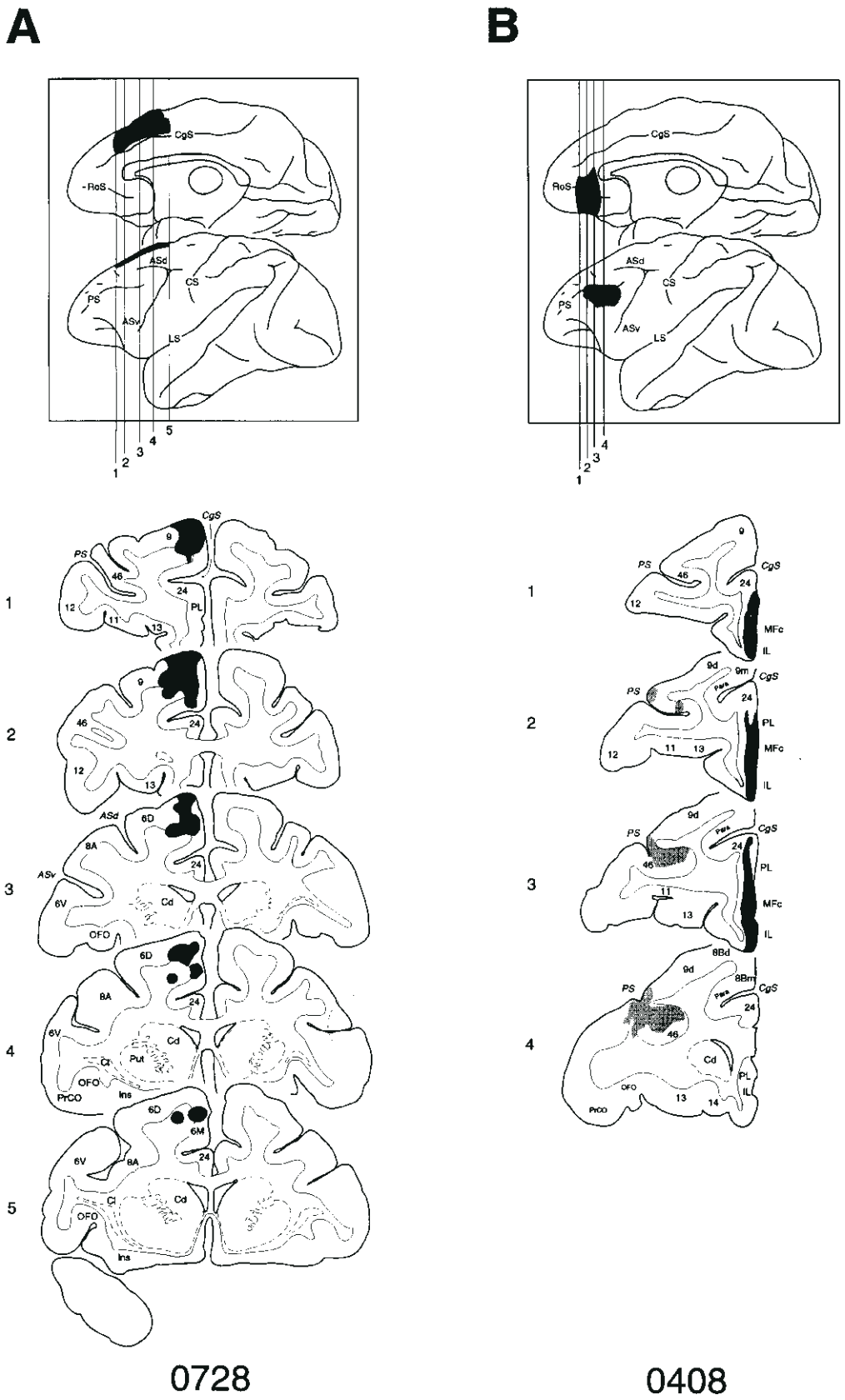

Figure 7. (*A*) Camera lucida drawings of coronal sections of the macaque frontal lobe from case 0728 illustrating a fast blue injection site in the region of the supplementary motor cortex (area 6M) and the granular frontal area 8B. The very caudal aspect of area 9d was also included in this site. (*B*) Camera lucida drawings of coronal sections of the macaque frontal lobe from case 0408 illustrating a fluororuby injection site (gray) in principal sulcus and a fast blue injection site in the medial frontal cortex. *Top*: Medial and lateral schematic views of the macaque cerebral cortex illustrating the anterior–posterior location of the coronal sections below. See text for details.

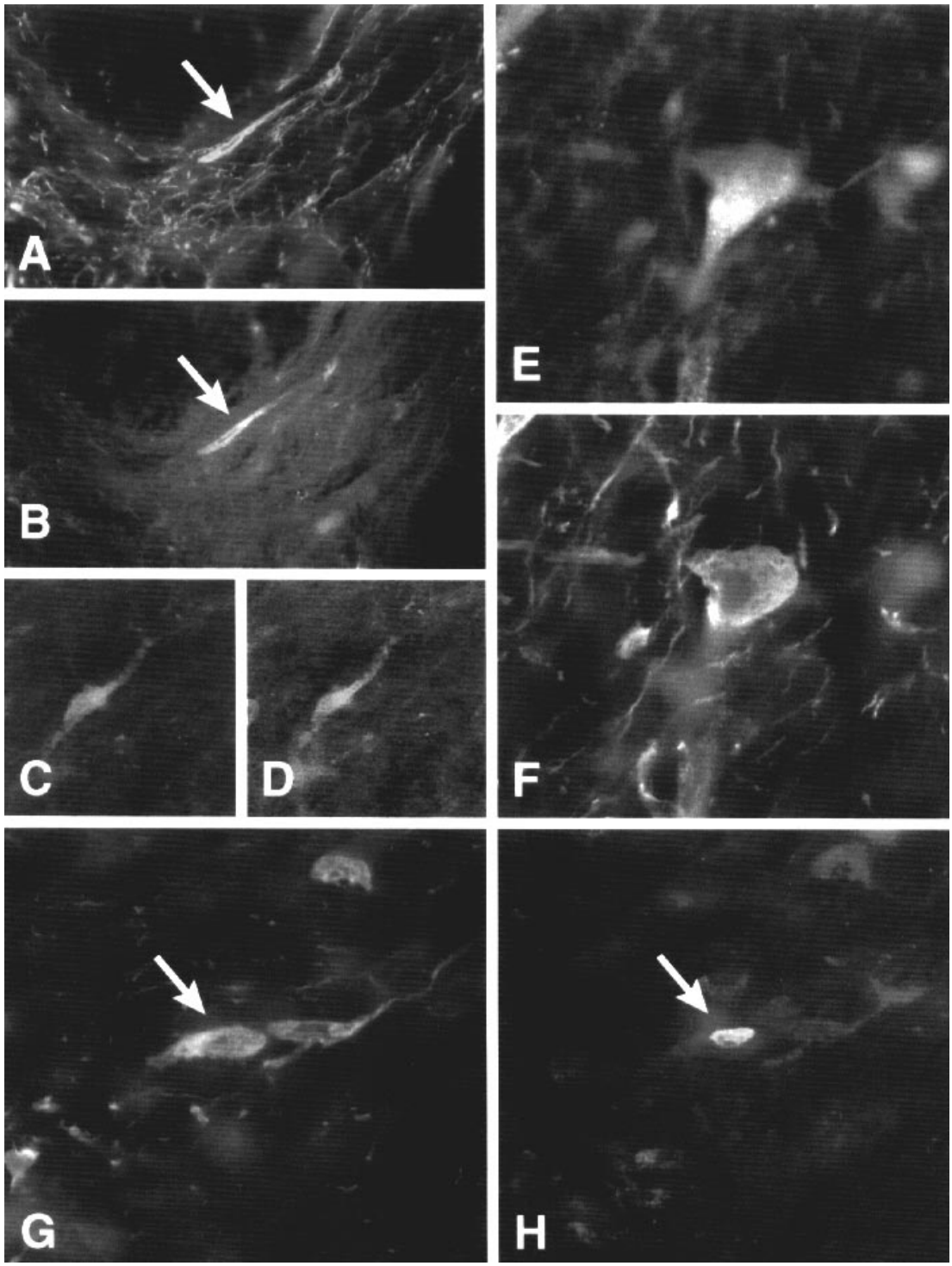

Figure 8. Photomicrographs of retrogradely labeled, tyrosine hydroxylase immunoreactive mesencephalic neurons that project to dorsal cortical areas. (*A*,*B*) A fast blue/TH area 46-projecting cell (arrows) located in the parabrachial pigmented nucleus of the VMT. (*C*,*D*) A fast blue/TH area 4-projecting cell (arrows) located in the A9 dorsalis region. (*E*,*F*) A fast blue/TH area 6M/8B-projecting cell located in the A9 dorsalis region. (*G*,*H*) A diamidino yellow/TH area 12-projecting neuron (arrows) located in the ventral portion of A9*d*.

(A8). In the present study we recognized several further subdivisions of these DA cell groups. We employed the nomenclature of Halliday and Tork (1986) in our analysis of the ventral mesencephalic tegmentum, in which five nuclei comprise this structure: two lateral nuclei, the large parabrachial pigmented nucleus (PBPG) and the paranigral nucleus (PN), which is located ventrally to PBPG, and three medial nuclei: two linear (the rostral [RLi] and central (or caudal) [CLi] components) and the interfascicular nucleus (IF) (Fig. 1). In the present study, we recognized two subdivisions of the A9 cell group: the densely packed DA cells of the substantia nigra pars compacta (SNpc) and a group of more loosely organized DA cells dorsal to the SNpc and lateral to the PBPG, referred to here as the A9 dorsalis (A9*d*) (Fig. 1). The A9*d* includes cells of the pars dorsalis of Poirier *et al.* (1983) and may share DA neurons of the dorsal aspect of the *pars mixta* of Francois *et al.* (1985). DA cells of this region

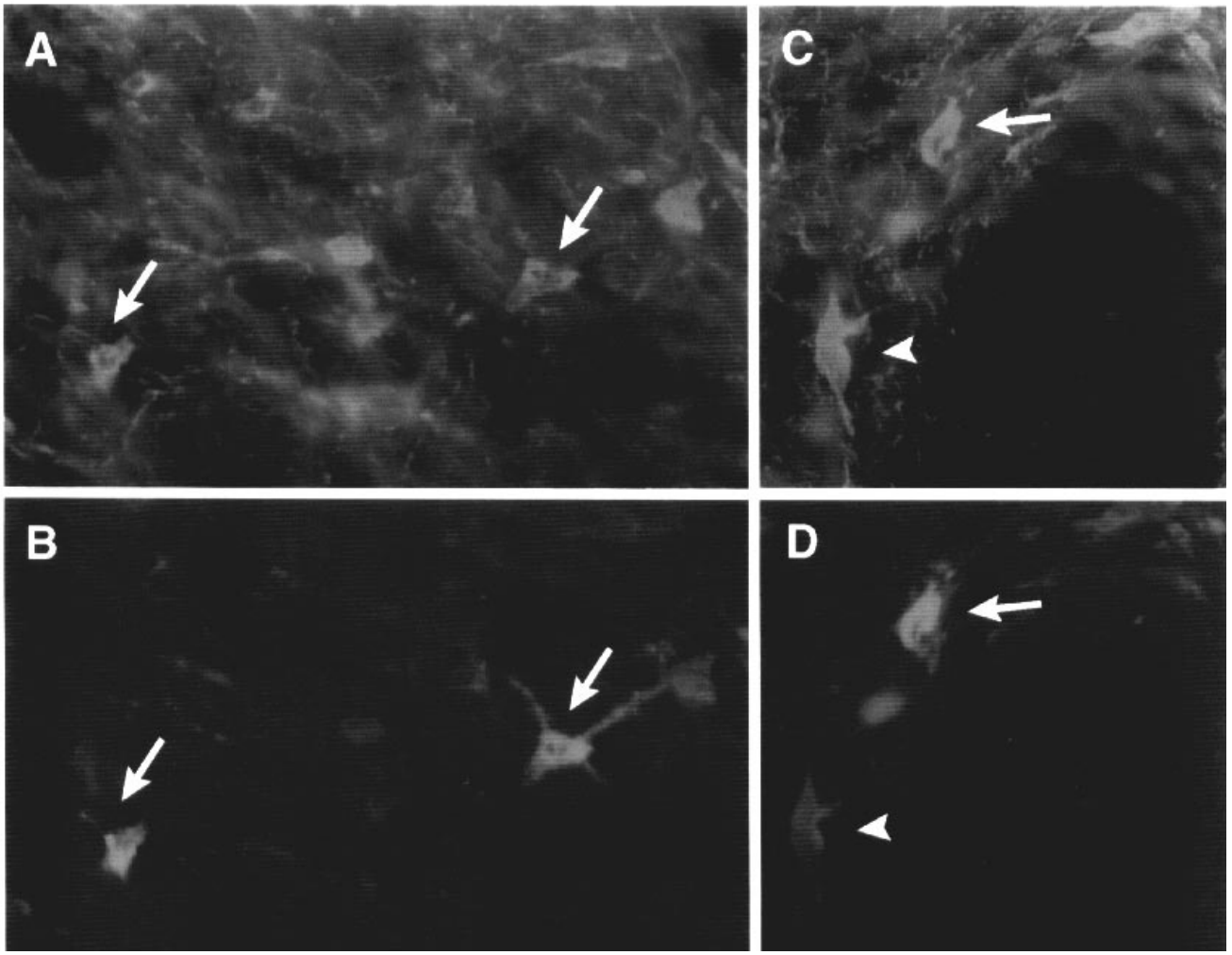

Figure 9. Photomicrographs of retrogradely labeled and tyrosine hydroxylase (TH)-immunoreactive mesencephalic neurons that project to medial frontal cortex. (*A*,*B*) A fast blue/TH anterior cingulate-projecting cell (arrows) observed in the caudal linear nucleus. (*C*,*D*) A fast blue/TH prelimbic area-projecting cell (arrows) located in the parabrachial pigmented nucleus of the VMT.

are considered to belong to PBPG in some classifications (Halliday and Tork, 1986; McRitchie *et al.*, 1996), whereas others do not distinguish this group from the SNpc (see Gaspar *et al.*, 1992). In the human mesencephalon, A9*d* is similar to the gamma subdivision of the SNpc in the nomenclature of Olszewski and Baxter (1954).

The A8 cell group is essentially a caudal extension of A9*d* and is easily recognizable at the level of the decussation of the superior cerebellar peduncle (Fig. 1*B*). These cells are distributed in the mesencephalic reticular formation in a region which corresponds to the retrorubral nucleus as recognized in carnivores (Rioch, 1948; Berman *et al.*, 1968). Medially, A8 neurons are continuous with the A10 PBPG and CLi cells and laterally with the A9 neurons of the substantia nigra pars lateralis. Many A8 neurons are scattered within and medial to the medial lemniscus (see Arsenault *et al.*, 1988). A dorsal cell dense component and more diffusely organized ventral component have been recognized in the primate (Deutch *et al.*, 1986). In addition to the A8-A10 DA neurons, several dopaminergic cells were observed in the ventral half of the periaqueductal gray in the rostral half of the midbrain. This DA cell group has been referred to as A*aq* and is continuous with the periventricular DA cells of the diencephalon (Felten and Sladek, 1983).

Data Analysis

Prior to coverslipping, 8 × 10 in. photographic images of the immunostained sections were generated. These photographs served as detailed maps of the mesencephalon and were used to plot the retrogradely labeled and immunostained neurons in relation to blood vessels, axonal tracts and other landmarks. Sections were analyzed on a Zeiss Axiophot fluorescence microscope**.** The distribution of all RL neurons and RL/TH immunoreactive cells was examined from the level of the mammillary bodies to the level of the locus coeruleus. Calbindin D_{28k}- and TH-immunostained adjacent sections, as well as those stained for Nissl and myelin, were used in the determination of the various subdivisions and nuclei of the ventral mesencephalon.

As the midbrain DA cells are distributed in a continuum, the boundaries between the cell groups A8, A9 and A10, as well as between the component nuclei of these groups, are for the most part indiscernible. This is particularly the case for the borders between the SNpc, the PBPG and the more loosely organized dopamine cells distributed in the mesencephalic reticular formation (A9*d*, A8). It is precisely in these regions that the vast majority of mesofrontal dopamine cells reside. Thus, to accurately assign each of these neurons to a specific VMT nucleus, or a subdivision of the substantia nigra or even to one of the three cell loci (A8–A10) is often a formidable task, which is further complicated by the fact that the nomenclature used by different researchers is quite varied, as is the assignment of A8–A10 loci. As the Dahlstrom and Fuxe (1964) scheme was derived from the study of the rodent and much subsequent work has been conducted in this species, comparisons to the primate also add complexity to this issue. In an effort to localize precisely the mesofrontal DA cells, we have presented the exact location of RL (i.e. non-TH) and RL/TH-immunoreactive neurons superimposed on

Figure 10. Distribution of retrogradely labeled (RL) and RL/tyrosine hydroxylase (TH)-immunoreactive neurons in the mesencephalon following injections of fast blue in the dorsolateral prefrontal cortex (area 46/9). The distribution of RL and RL/TH-immunoreactive neurons is presented on adjacent cresyl violet-stained sections to demonstrate the relationship between the RL neurons and midbrain cell groups. Sections are arranged in rostral–caudal order (*A* is most rostral). See bottom of figure for symbol legend. Each symbol represents one neuron. (*A*,*B*) Numerous RL, non-TH-immunoreactive neurons were observed in the rostral mesencephalon. (*C*,*D*) At the level of the third nerve rootlets and red nucleus, area 46-projecting DA neurons (RL/TH) are primarily located in A9*d* and PBPG. (*E*,*F*) At the level of the DSCP, numerous RL/TH-immunoreactive neurons were observed in the A8 region. (*G*) In more caudal sections of the midbrain, a few RL/TH neurons were observed in the retrorubral field. (*H*) Numerous RL/TH, presumably noradrenergic cells were located in the locus coeruleus.

Figure 11. Distribution of retrogradely labeled (RL) and RL/tyrosine hydroxylase (TH)-immunoreactive neurons in the mesencephalon following injections of fast blue (area 46) and diamidino yellow (area 12) in the dorsolateral prefrontal cortex. The distribution of RL and RL/TH-immunoreactive neurons is presented on adjacent TH-immunolabeled sections to demonstrate the relationship between the RL neurons and midbrain cell groups. Sections are arranged in rostral–caudal order (*A* is most rostral). See bottom of figure for symbol legend. Each symbol represents one neuron. (*A*,*B*) Numerous RL, non-TH-immunoreactive neurons were observed in the rostral mesencephalon, some of which contained both fluorochromes (*A*). (*C*,*D*) At the level of the third nerve rootlets and red nucleus, area 46-projecting DA neurons (RL/TH) are primarily located in A9*d* and PBPG. Area 12-projecting neurons were typically observed ventral to those innervating area 46. (*E*,*F*) At the level of the DSCP, numerous RL/TH-immunoreactive neurons were observed in the A8 region. Again, area 12-projecting neurons were observed ventrally to area 46-projecting cells. (*G*) In the caudal midbrain, numerous area 46-projecting neurons were observed in the retrorubral area (A8). (*H*) Few RL/TH neurons were observed at more caudal levels.

Figure 12. Distribution of retrogradely labeled (RL) and RL/tyrosine hydroxylase (TH)-immunoreactive neurons in the mesencephalon following injections of fast blue in the medial prefrontal cortex (area PL). The distribution of RL and RL/TH-immunoreactive neurons is presented on adjacent sections which were stained for TH immunoreactivity (DAB) to demonstrate the relationship between the RL neurons and DA cell groups. See bottom of figure for symbol legend. Each symbol represents one neuron. (*A*) Numerous RL, non-TH-immunoreactive neurons were observed in the rostral mesencephalon. (*B–D*) In the rostral mesencephalon, RL/TH neurons are primarily located in the PBPG and rostral linear nucleus. (*E*) Numerous PL-projecting neurons are observed in the rostral A8 region. (*F*) At the level of the DSCP, numerous RL/TH-immunoreactive neurons were observed in the VMT caudal linear nucleus. (*G*) In the caudal midbrain, most RL/TH neurons were observed in the caudal linear nucleus. (*H*) A few RL/TH, presumably noradrenergic cells, were located in the locus coeruleus.

Figure 13. Distribution of retrogradely labeled (RL) and RL/tyrosine hydroxylase (TH)-immunoreactive neurons in the mesencephalon following injections of fast blue in the anterior cingulate cortex (area 24). The distribution of RL and RL/TH-immunoreactive neurons is presented on adjacent sections which were stained for TH immunoreactivity (DAB) to demonstrate the relationship between the RL neurons and DA cell groups. See bottom of figure for symbol legend. Each symbol represents one neuron. (*A*) Numerous RL, non-TH-immunoreactive neurons were observed in the rostral mesencephalon. (*B–D*) At the level of the red nucleus, RL/TH neurons are primarily located in the PBPG and A9*d*. (*E*) Numerous area 24-projecting neurons are observed in A9*d* and the rostral A8 region. (*F*,*G*) At the level of the DSCP, RL/TH-immunoreactive neurons were observed in the VMT caudal linear nucleus and A8, particularly the medial aspect of the retrorubral area. (*H*) Few RL/TH neurons were observed at more caudal levels.

Figure 14. Distribution of retrogradely labeled (RL) and RL/tyrosine hydroxylase (TH)-immunoreactive neurons in the mesencephalon following injections of fast blue in the dorsomedial prefrontal/precentral cortex (area 8B/6M). The distribution of RL and RL/TH-immunoreactive neurons is presented on adjacent sections which were stained for TH immunoreactivity (DAB) to demonstrate the relationship between the RL neurons and DA cell groups. Sections are arranged in rostral–caudal order (*A* is most rostral). See bottom of figure for symbol legend. Each symbol represents one neuron. (*A*,*B*) Some RL, non-TH-immunoreactive neurons were observed in the rostral mesencephalon. RL/TH neurons at this level were observed in the PBPG and RL nuclei. (*C*,*D*) At the level of the third nerve rootlets and red nucleus, area 8B/6M-projecting DA neurons are primarily located in A9*d* and the PBPG. (*E*,*F*) At the level of the DSCP, numerous RL/TH-immunoreactive neurons were observed in the A8 region. (*G*) In more caudal midbrain sections, RL/TH neurons were densely distributed in the retrorubral field. (*H*) Few RL/TH neurons were observed at more caudal levels.

Figure 15. Distribution of retrogradely labeled (RL) and RL/tyrosine hydroxylase (TH)-immunoreactive neurons in the rostral mesencephalon following injections of fast blue in the dorsal precentral cortex (area 4). The distribution of RL and RL/TH-immunoreactive neurons is presented on adjacent sections which were stained for TH immunoreactivity (DAB) to demonstrate the relationship between the RL neurons and DA cell groups. Sections are arranged in rostral–caudal order (*A* is most rostral). See bottom of figure for symbol legend. Each symbol represents one neuron. (*A*,*B*) Several RL, non-TH-immunoreactive neurons were observed in the rostral mesencephalon. (*C*,*D*) At the level of the third nerve rootlets and red nucleus, area 8B/6M-projecting DA neurons (RL/TH) are primarily located in A9*d* and the lateral PBPG. (*E*,*F*) At the level of the DSCP, numerous RL/TH-immunoreactive neurons were observed in the A8 region and A9*d*. A few area 4-projecting neurons were observed in the lateral and ventral A9 regions. (*G*,*H*) In more caudal midbrain sections, RL/TH neurons were distributed in the dorsal retrorubral field.

low-power photomicrographs of adjacent serial sections stained for TH or for Nissl substance (Figs 10–16).

Results

Injection Sites

In this study, the retrograde fluorochrome fast blue was utilized to label mesencephalic neurons projecting to motor, premotor and prefrontal cortices. Other retrograde fluorochromes were employed as well, including diamidino yellow, fluorogold and fluororuby. As mentioned above (see Materials and Methods), these fluorochromes provided adequate retrograde transport to the thalamus; however, in general, transport to the midbrain was insufficient for thorough analysis. Therefore, with the exception of two double-label cases in which a diamidino yellow or fluororuby injection was made in addition to a fast blue injection, the results of these injections will not be discussed.

In all cases, the injection sites were confined to the cortical gray matter, often covering the entire cortical depth. Figure 2 schematically illustrates the locations of all of the injection sites in the present study in reference to the cytoarchitectonic areas of the frontal lobe as defined by Preuss and Goldman-Rakic (1991). Figures 4–7 illustrate the full extent of selected cortical injections. Sulcal landmarks and adjacent serial coronal sections stained for Nissl substance were used to determine the cytoarchitectonic areas injected.

Dorsolateral Granular Frontal (Prefrontal) Injections

Cases 1116, 1218, 0902 contain injections of fast blue in the dorsolateral granular frontal (prefrontal) cortex. The injection site in case 1116 is considerably smaller than 0921 and is primarily confined to the ventral rim of the principal sulcus (see Fig. 2). A similarly small injection was made in area 8Bd in case 1218 (see Fig. 2). A much larger injection was made in the

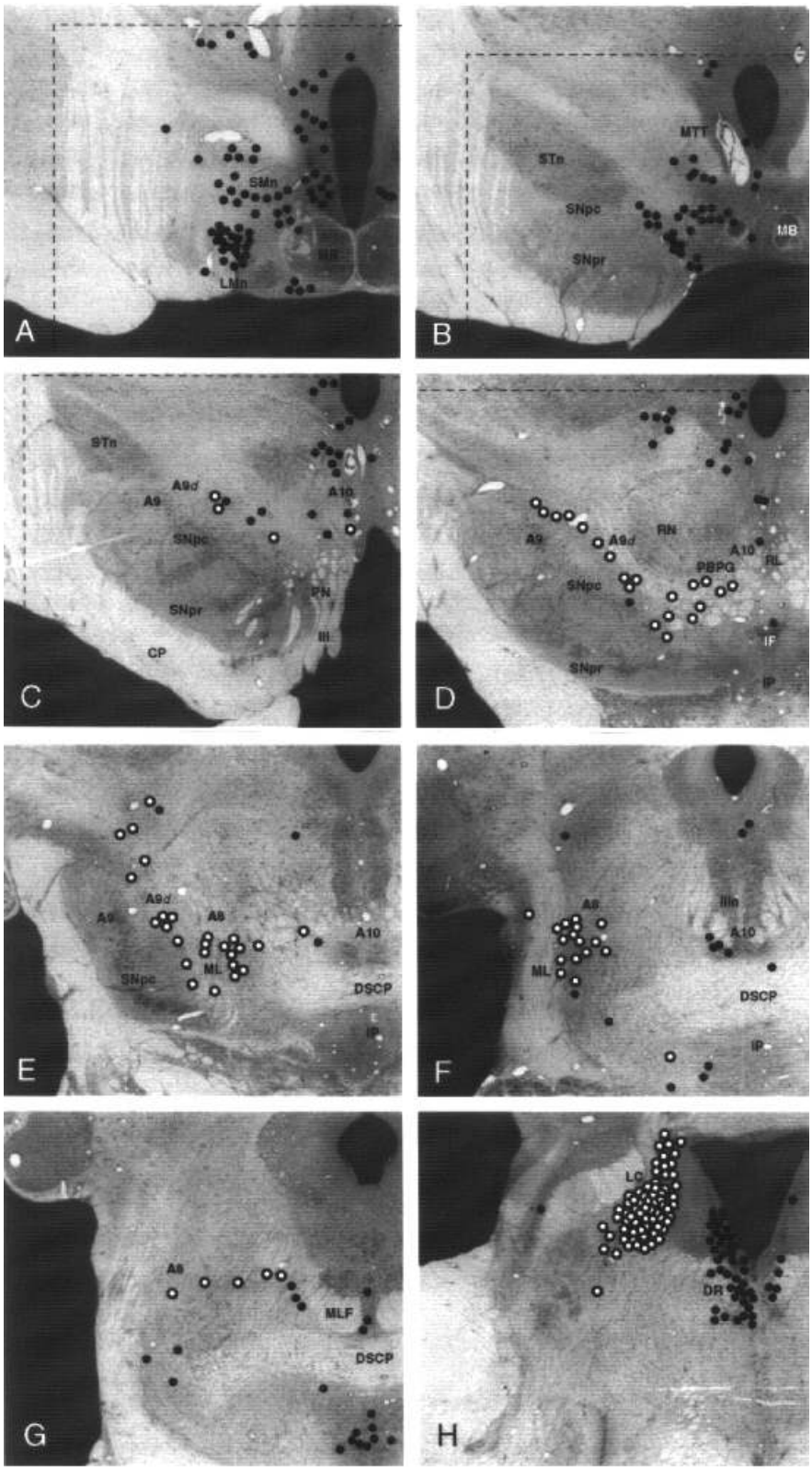
A
SMn
LMn
MB
B
MTT
STn
SNpc
SNpr
MB
C
STn
A9d
A9
A10
SNpc
SNpr
PN
III
CP
D
A9
A9d
RN
A10
RL
PBPG
SNpc
IF
SNpr
IP
E
A9d
A9
A8
A10
ML
SNpc
DSCP
IP
F
A8
IIIn
A10
ML
DSCP
IP
G
A8
MLF
DSCP
H
LC
DR
0902 Dorsolateral Granular Frontal (Area 46)
fast blue +
fast blue / tyrosine hydroxylase +

Figure 10

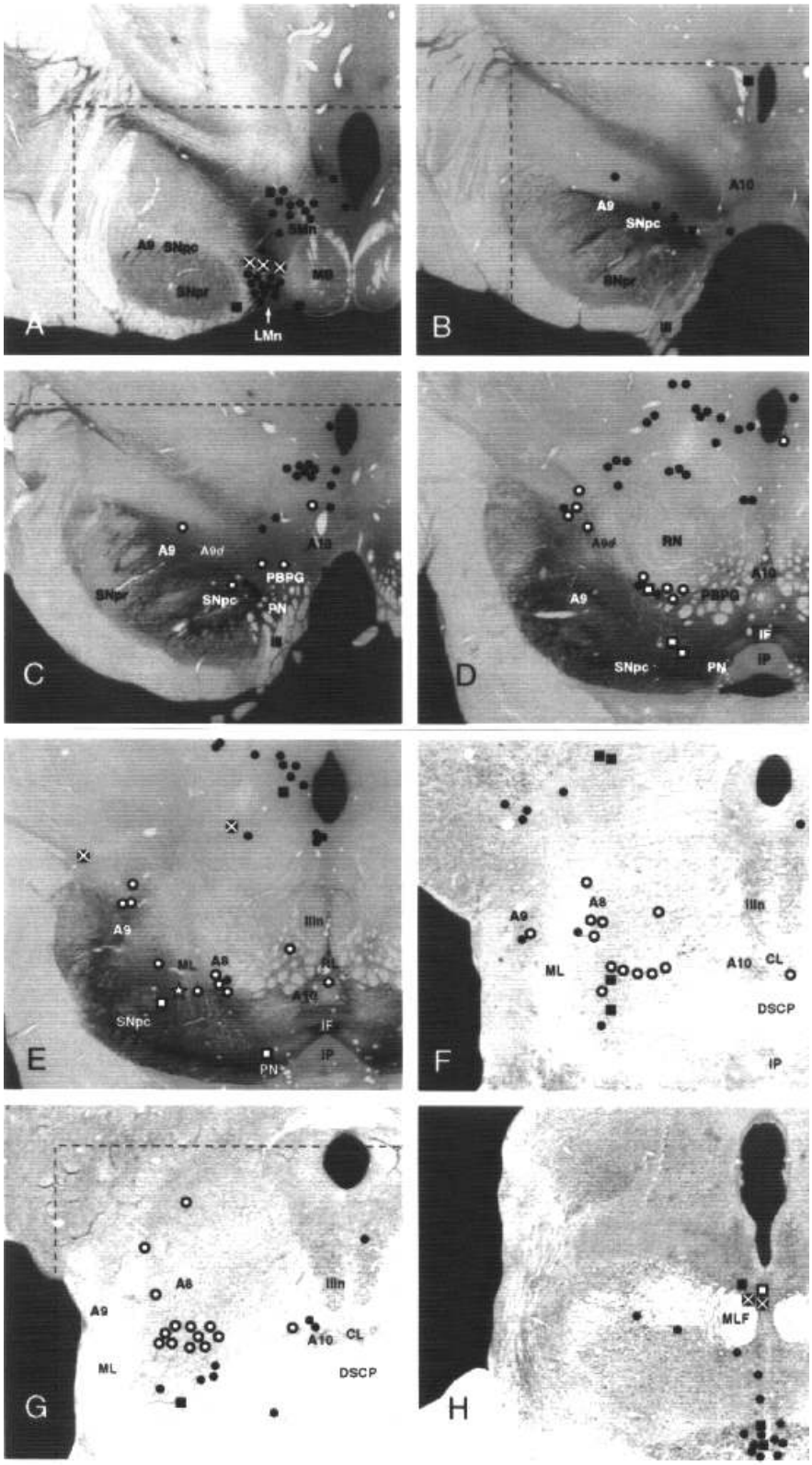

0921 Dorsolateral Granular Frontal
(Area 46 [FB] & Area 12 [DY])

- ● fast blue +
- ■ diamidino yellow +
- ⊠ fast blue / diamidino yellow +
- ○ fast blue / tyrosine hydroxylase +
- □ diamidino yellow / tyrosine hydroxylase +

Figure 11

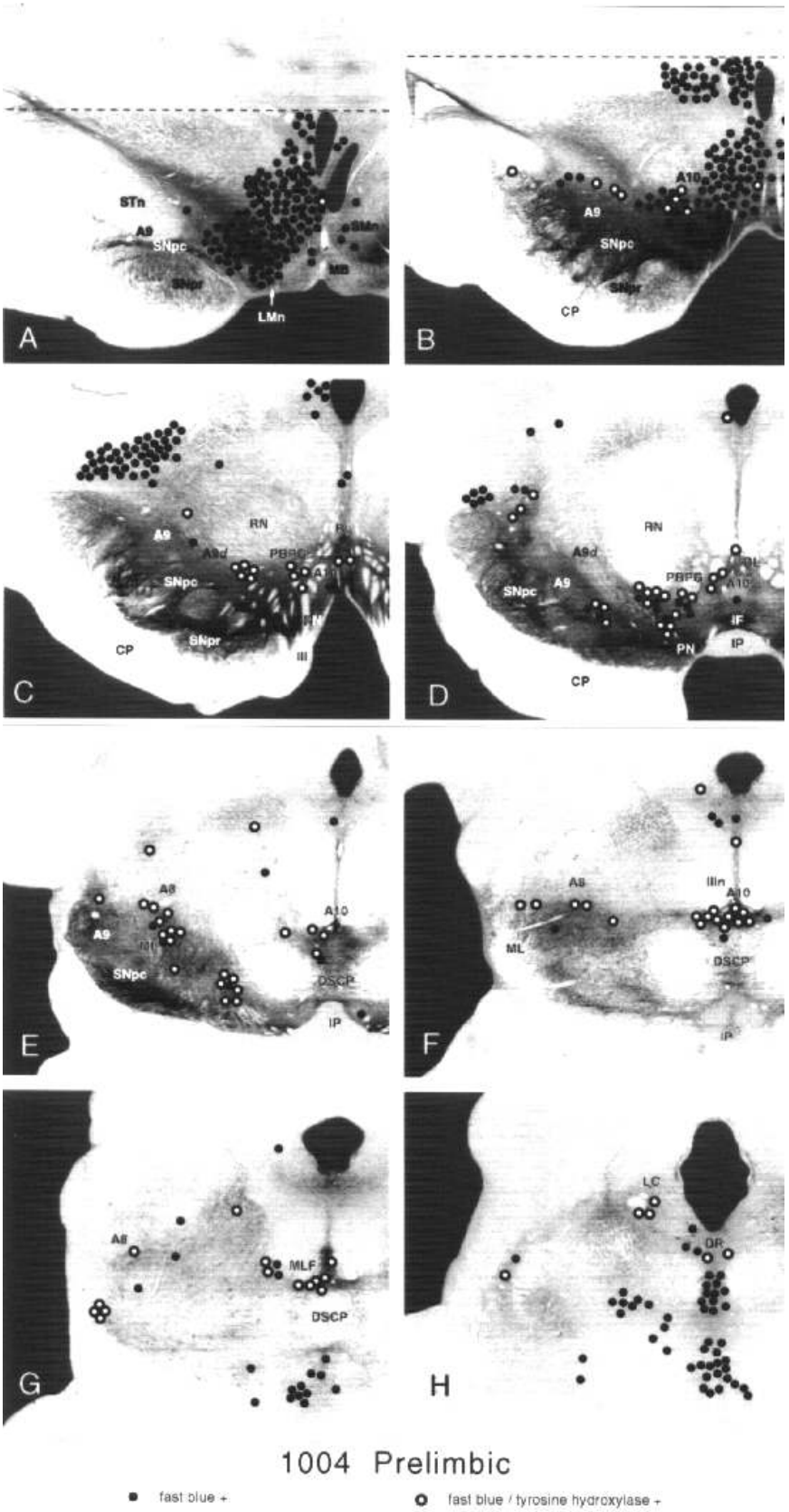
STn
A9
SNpc
SNpr
LMn
MD
A
A10
A9
SNpc
SNpr
CP
B
RN
A9
A9d
PBPC
SNpc
SNpr
CP
III
C
RN
A9d
PBPC
A9
SNpc
PN
IP
CP
D
A8
A9
A10
SNpc
DSCP
IP
E
A8
IIIn
A10
ML
DSCP
IP
F
A8
MLF
DSCP
G
LC
DR
H
1004 Prelimbic
fast blue +
fast blue / tyrosine hydroxylase +

Figure 12

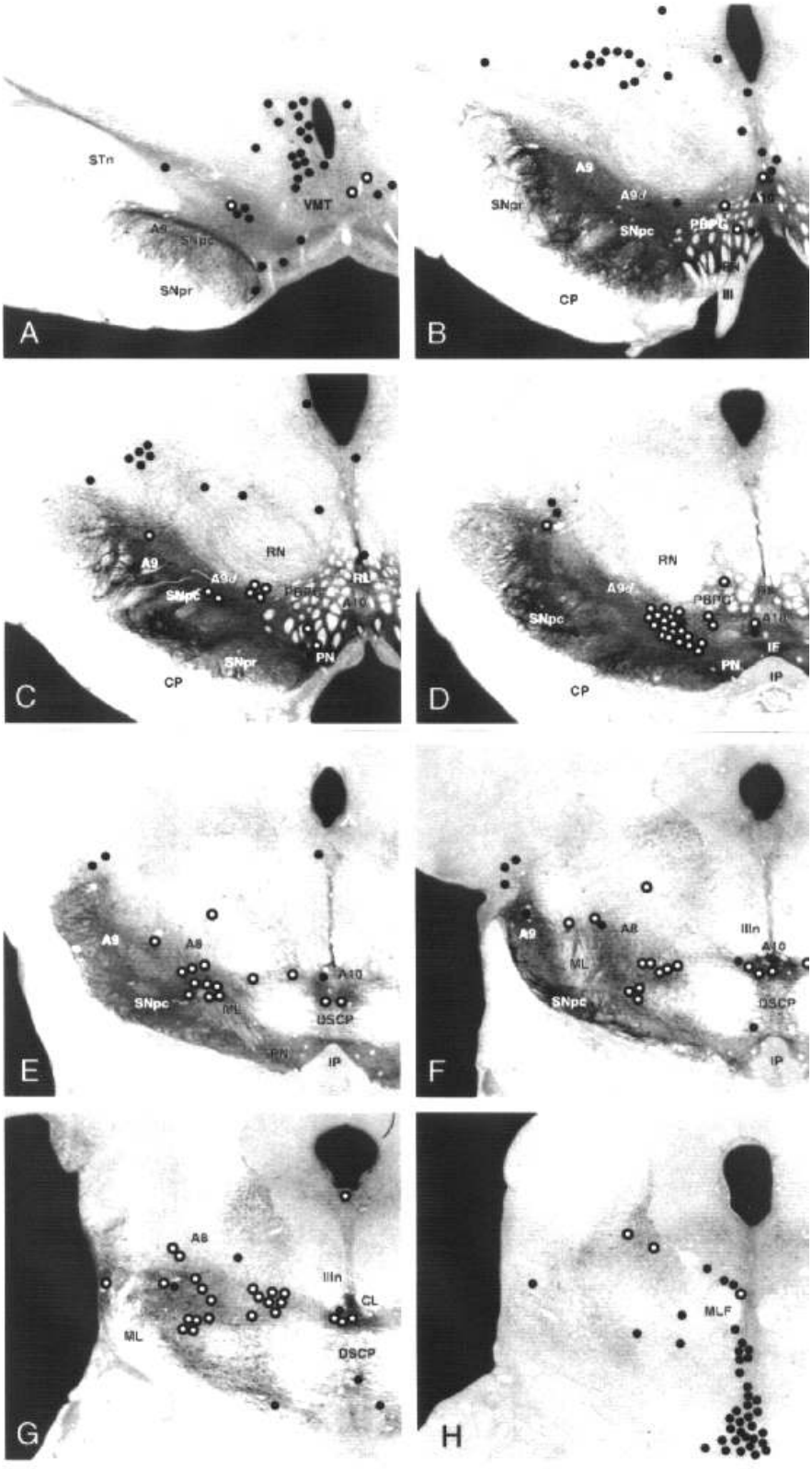
STn
VMT
A8
SNpc
SNpr
A
A9
A9d
SNpr
SNpc
A10
III
CP
B
RN
RL
PBPC
PN
IF
IP
C
D
ML
IIIn
DSCP
E
F
CL
MLF
G
H
0206 Cingulate
fast blue +
fast blue / tyrosine hydroxylase +

Figure 13

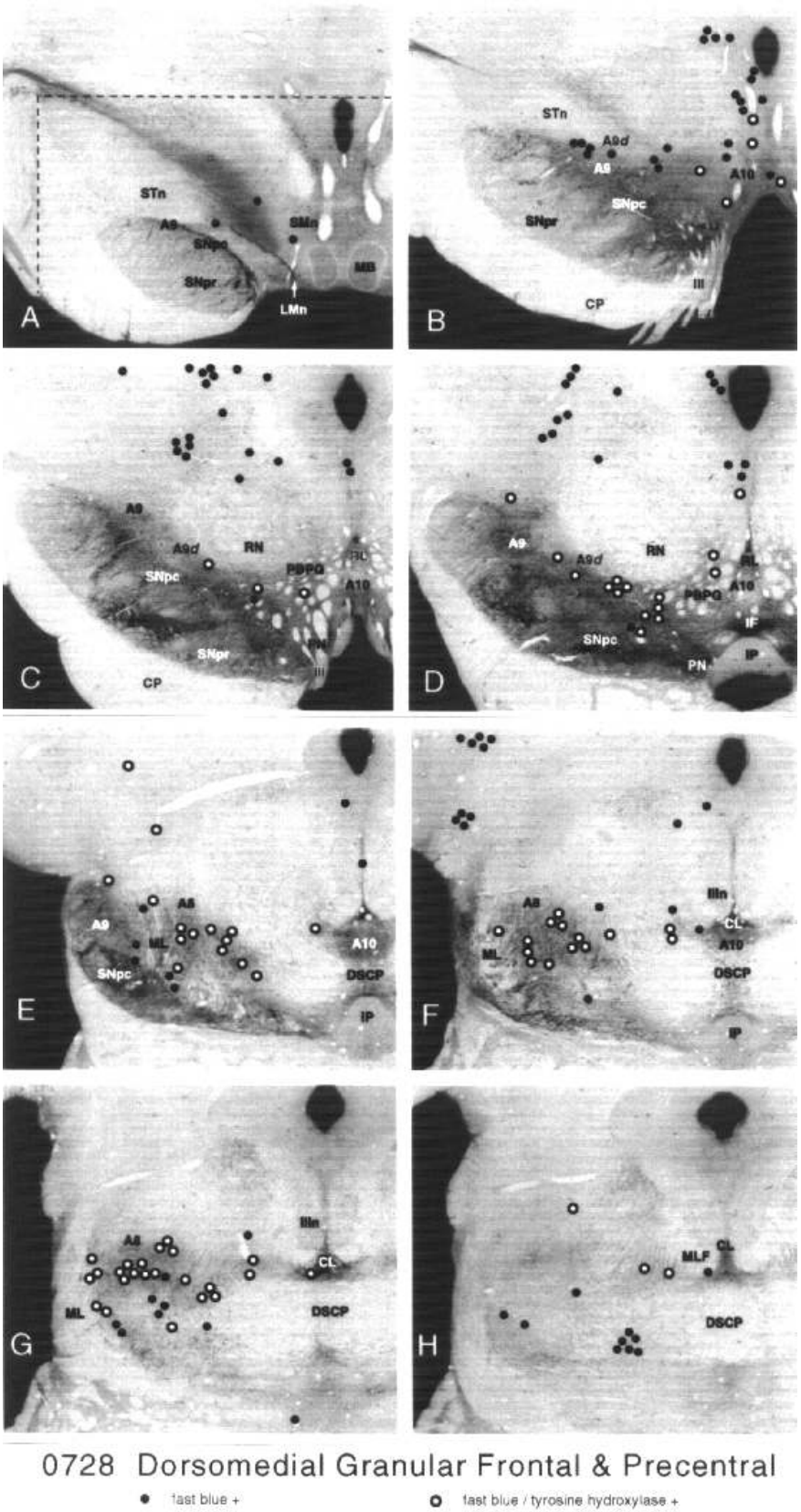
A
STn
A8
SNpc
SNpr
SMn
LMn
MB
B
STn
A9d
A8
A10
SNpc
SNpr
III
CP
C
A8
A9d
RN
SNpc
PBPQ
RL
A10
SNpr
PN
III
CP
D
A9
A9d
RN
RL
A10
PBPQ
IF
SNpc
PN
IP
E
A8
A9
ML
A10
SNpc
DSCP
IP
F
A8
IIIn
CL
A10
ML
DSCP
IP
G
IIIn
A8
CL
ML
DSCP
H
MLF
CL
DSCP
0728 Dorsomedial Granular Frontal & Precentral
fast blue +
fast blue / tyrosine hydroxylase +

Figure 14

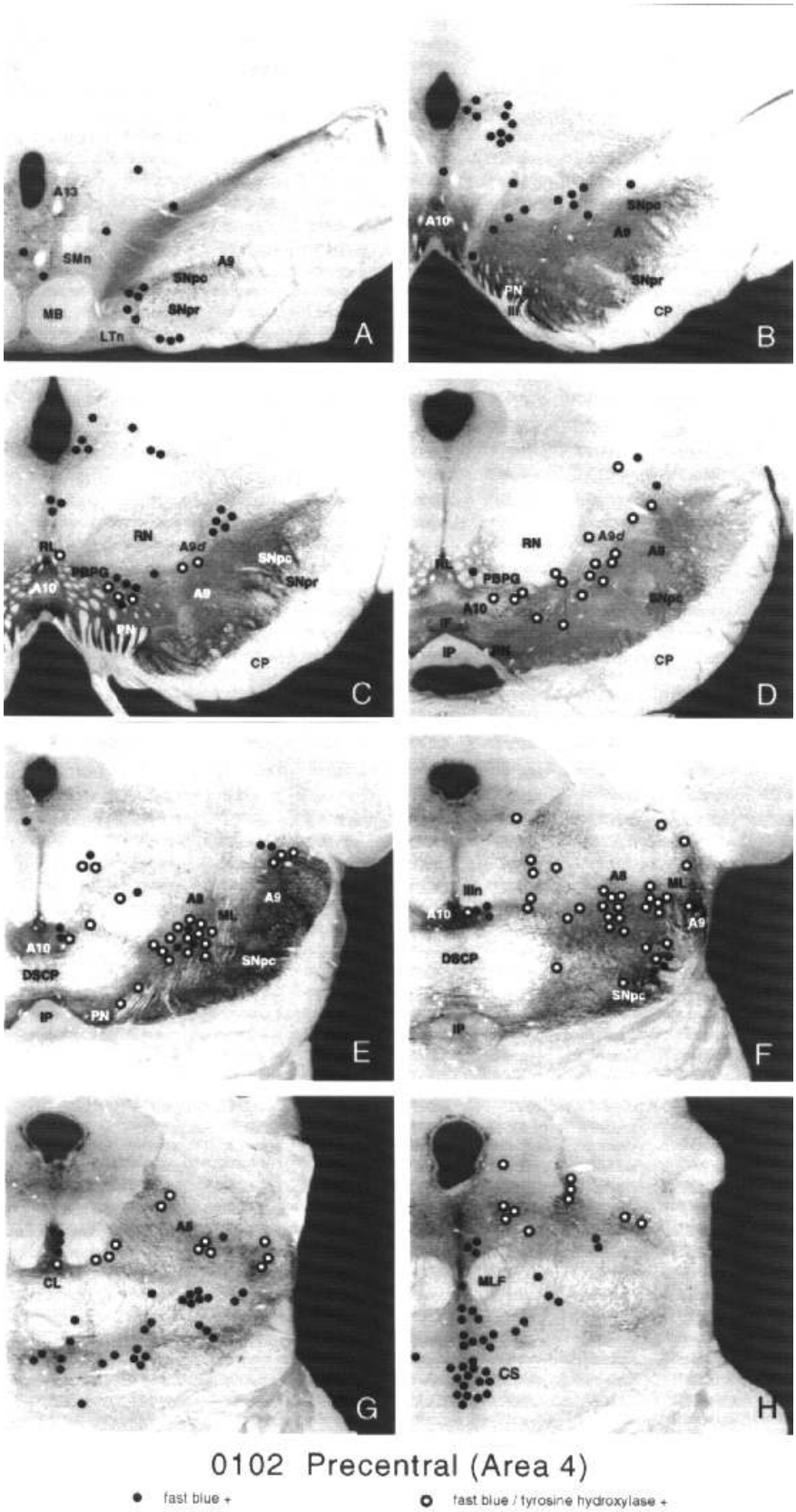
A13
SMn
MB
LTn
A9
SNpc
SNpr
A
A10
SNpc
A9
SNpr
PN
III
CP
B
RL
RN
A9d
SNpc
SNpr
A10
PBPG
A9
PN
CP
C
RN
A9d
A9
RL
PBPG
SNpc
A10
IF
IP
PN
CP
D
A9
A9
ML
A10
SNpc
DSCP
IP
PN
E
IIIn
A9
ML
A10
A9
DSCP
SNpc
IP
F
A9
CL
G
MLF
CS
H
0102 Precentral (Area 4)
fast blue +
fast blue / tyrosine hydroxylase +

Figure 15

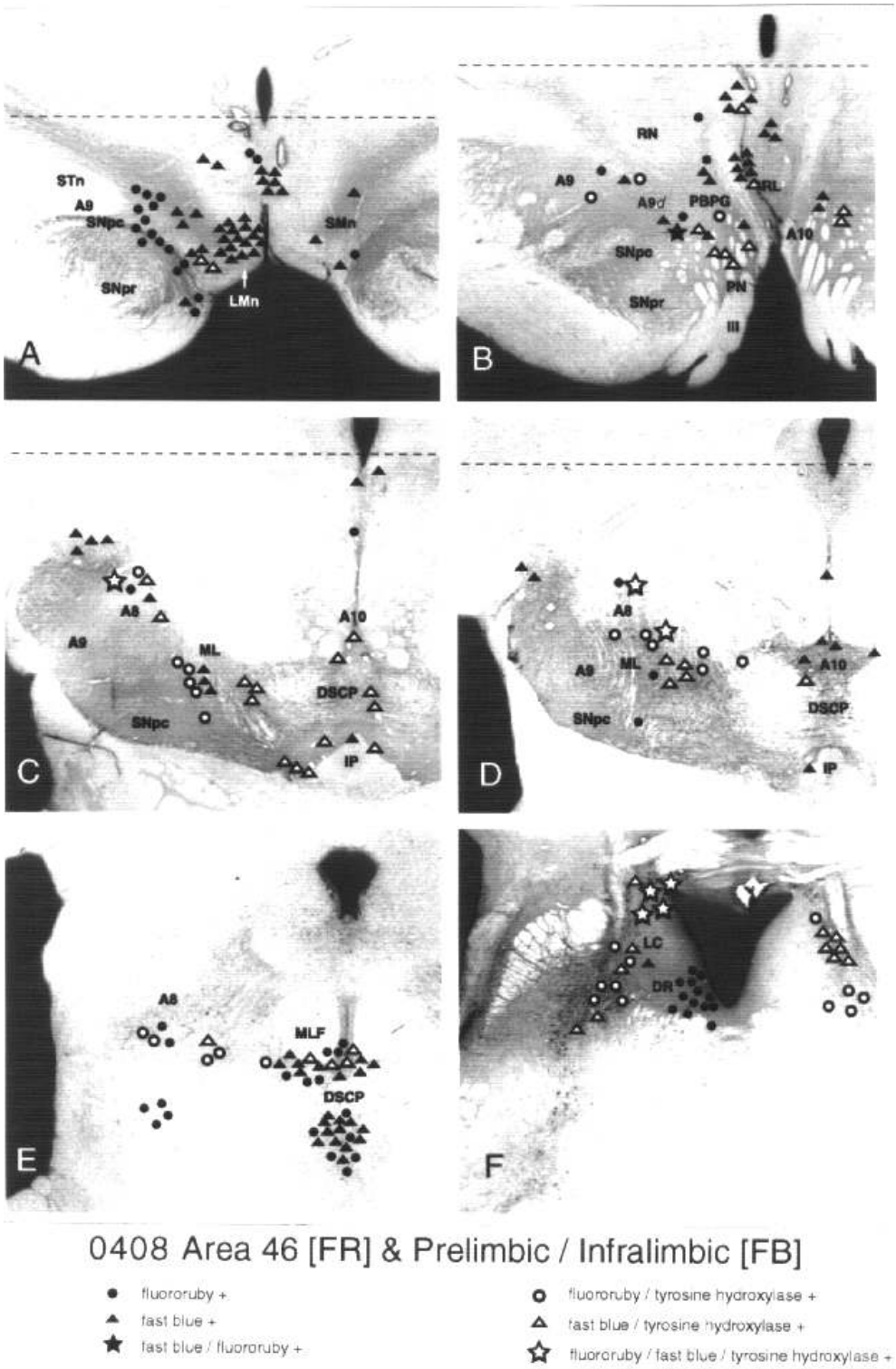

Figure 16. Distribution of retrogradely labeled (RL) and RL/tyrosine hydroxylase (TH)-immunoreactive neurons in the mesencephalon following injections of fluororuby into the principal sulcus (area 46) and fast blue in the medial prefrontal cortex (areas PL and IL). The distribution of RL and RL/TH-immunoreactive neurons is presented on adjacent sections which were stained for TH immunoreactivity (DAB) to demonstrate the relationship between the RL neurons and DA cell groups. See bottom of figure for symbol legend. Each symbol represents one neuron. (*A*) Numerous RL, non-TH-immunoreactive neurons were observed in the rostral mesencephalon, some of which contained both retrograde fluorochromes. (*B*) In the rostral mesencephalon, FR/TH neurons are primarily located in the dorsal lateral and A9d, whereas the FB/TH neurons were observed in the PBPG and rostral linear nucleus. (*C*,*D*) At the level of the DSCP, a clear segregation of dorsolateral and medial PFC-projecting DA neurons is evident, with only a few TH-immunoreactive neurons demonstrating both retrograde fluorochromes. (*E*) In the caudal midbrain, most FB/TH neurons were observed in the caudal linear nucleus, whereas FR/TH neurons were located laterally in the A8 region (*F*) Numerous FR/TH and FB/TH, presumably noradrenergic cells were located in the locus coeruleus. Many of these cells possessed both retrograde fluorochromes.

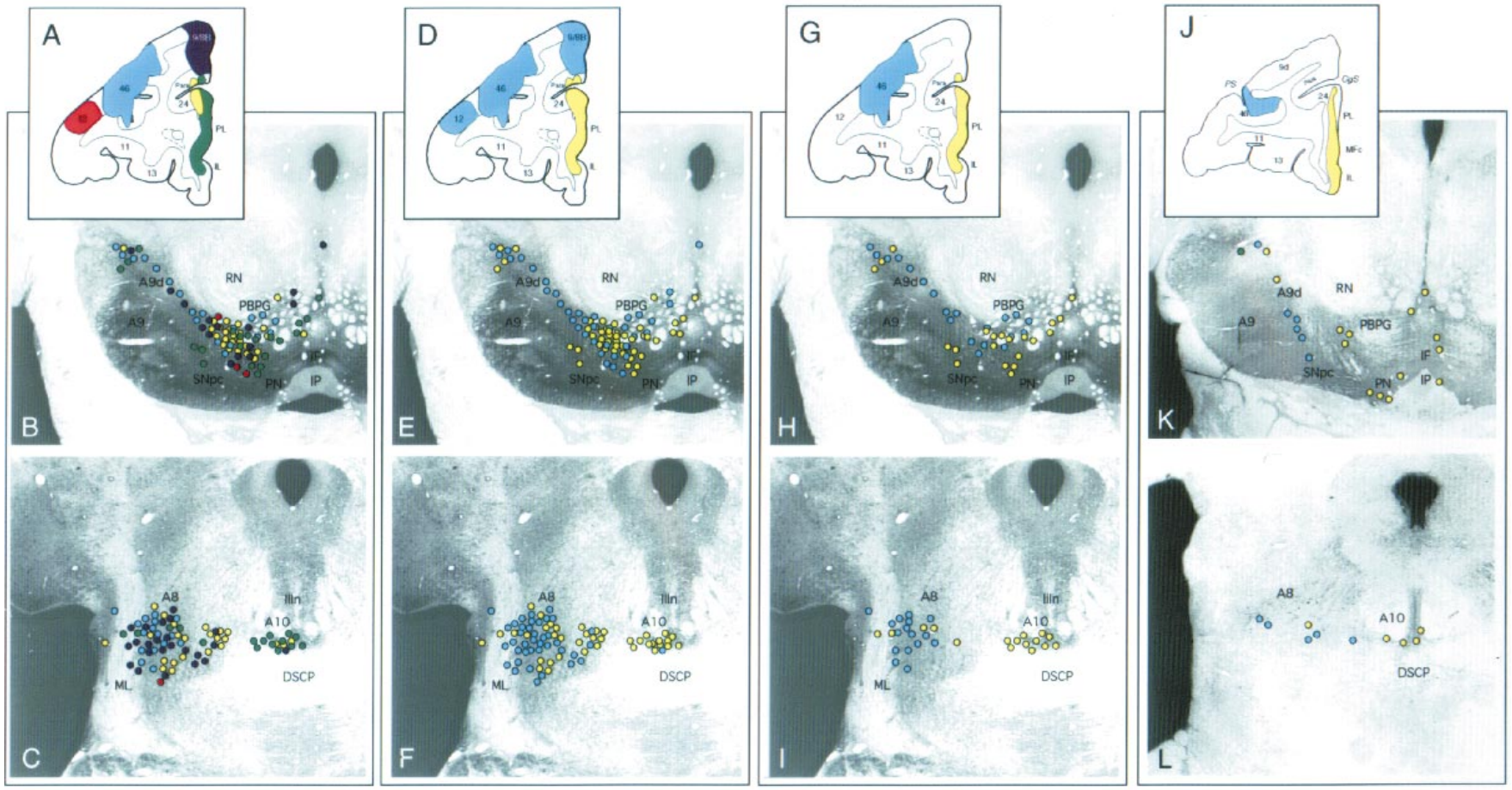

Figure 17. Composite figure of injection sites and retrogradely labeled dopaminergic neurons from five cases in the present study (*A–I*) compared with the distribution of retrogradely labeled dopaminergic neurons from case 0408 (*J–L*) illustrating the topographic organization of the mesofrontal dopamine system. Each circle represents one neuron. (*A*) Anterior coronal section of the macaque frontal cortex illustrating the five injection sites, i.e. the cortical targets of the cells plotted below. (*B,C*) Composite figures illustrating the location of dopamine neurons innervating the five areas shown above. The cells from each case were plotted on representative rostral (*B*) and caudal (*C*) midbrain sections according to various morphological landmarks (nuclei, axonal tracts, etc.). A crude medio-lateral topography is evident; however, extensive overlap of the DA cells innervating the five areas is observed, especially in the PBPG. (*D*) The same injection sites as depicted in (*A*), grouped as either dorsal (blue) or ventromedial (yellow). (*E,F*) Comparison of the distribution of midbrain DA neurons innervating dorsal (blue) or ventromedial (yellow) frontal areas. As for (*B*) and (*C*), retrogradely labeled cells from each case were plotted on representative rostral (*E*) and caudal (*F*) midbrain sections. DA cells innervating the dorsal areas are situated lateral to those projecting to the ventromedial areas. In the caudal midbrain (*F*), dorsal cortical-projecting DA cells are located predominantly in the lateral half of A8, whereas the ventromedial neurons are located mostly in the caudal linear nucleus and medial A8. The majority of DA cells in the medial A8 region are area 24 projecting cells (*C*). (*G–I*) Composite figure of injection sites and retrogradely labeled midbrain cells from cases 0902 and 1004 illustrating the distribution of DA neurons innervating the dorsolateral vs. the medial prefrontal cortices. (*G*) Coronal section of the macaque frontal lobe illustrating the injection sites in the dorsolateral (area 46/9) and dorsomedial prefrontal cortex (PL). (*H,I*) Distribution of dopamine neurons innervating the dlPFC and mPFC areas shown above. The cells from each case were plotted on representative rostral (*H*) and caudal (*I*) midbrain sections. In the rostral midbrain, a crude mediolateral topography is evident; however, the distribution of DA cells innervating these two areas overlaps, especially in the PBPG. In the caudal midbrain, evidence of mediolateral topography is more obvious, such that DA cells innervating the dorsal areas are situated lateral to those projecting to the ventromedial areas. (*J*) Coronal section of the macaque frontal lobe illustrating the injection sites in case 0408 in which different fluorochromes were injected in the dorsolateral (area 46) and medial prefrontal cortex (PL/IL). (*K,L*) Topographic segregation of dorsolateral and medial prefrontal DA projections.

principal sulcal region of case 0902 involving both banks of the principal sulcus and the lateral edge of area 9 (Fig. 5*A*). Cases 0921 and 0408 each contain injections of two different retrograde tracers. In case 0921 (Fig. 5*B*), the fast blue injection site involves area 46, primarily the dorsal bank of the principal sulcus (PS) rostrally and extends caudally beyond the PS into area 8A. Diamidino yellow was also injected in the dorsal aspect of area 12vl in the same animal. Case 0408 contains a fluoruby injection extending into both banks of the middle two-thirds of the principal sulcus (Fig. 7*B*). A fast blue injection into the medial wall, ventral to the cingulate sulcus, also was made in this animal (see below for details).

Medial Prefrontal Injections

The PL [Walker's (1940) area 24/25] and anterior cingulate cortex (area 24, Preuss and Goldman-Rakic, 1991) were injected in case 1004 (Fig. 4*A*) using MRI to guide the stereotaxic injections. This injection site is located predominantly anterior to the genu of the corpus callosum, bound dorsally by cingulate sulcus and ventrally by the rostral sulcus. The medial frontal area (area MFc, Preuss and Goldman-Rakic, 1991; part of Walker's area 25), the dorsal aspect of the IL (area 25) and the ventromedial paralimbic cortex also were included in this injection site. In case 0206 (Fig. 4*B*), the fast blue injection site was centered ventral to the cingulate sulcus, in the anterior cingulate cortex (area 24b). This injection site involves a small portion of the paralimbic cortex. As described above, case 0408 contained a fast blue injection in the PL and IL cortices (Fig. 7*B*) in addition to the fluoruby injection in the dorsal granular frontal cortex. The fast blue site also included area MFc as well, thus forming a continuous dorsal-ventral zone of labeling extending from the ventral border of area 24 to the ventromedial tip of the cortex.

Precentral Injections

Two cases had injections caudal to the prefrontal cortex in the premotor (case 0728) or motor (case 0102) areas. In case 0728, a fast blue injection was made in a region containing the precentral area 6M, roughly equivalent to the supplementary motor area, and the rostral granular frontal areas 8B and 9 (Fig. 7*A*). This dorsomedial frontal region contains the highest density of dopaminergic-immunoreactive axons in the macaque neocortex (Williams and Goldman-Rakic, 1993). The injection site is localized to both the dorsal and medial aspects of area 6M and 8B (8Bd and 8Bm) as well as the caudal border of 9m. This injection is therefore centered in the dorsomedial precentral cortex but does include some dorsomedial granular frontal cortex. The dorsomedial aspect of the primary motor cortex, area 4 (M1), was injected with fast blue in case 0102 (Fig. 4). This injection site is located in an aspect of M1 roughly corresponding to the leg representation. This area is also densely innervated by DA axons in the macaque brain (Williams and Goldman-Rakic, 1993).

Distribution of Dopaminergic Neurons Projecting to the Frontal Cortex

Retrograde fluorochrome injections in each of the areas examined yielded numerous RL/TH immunoreactive (i.e. double labeled) cells in all three of the mesencephalic dopaminergic cell groups (A9, A10 and A8). The incomplete filling of neuronal somata and processes with the retrograde fluorochromes and immunofluorescence did not allow for precise analysis of mesofrontal DA cellular morphology. RL/TH cells exhibited a wide range of sizes and morphologies (Figs 8 and 9). Many mesofrontal DA neurons were fusiform (Fig. 8*A*,*B*), but others were oval (Fig. 9*C*,*D*) or triangular shaped (Fig. 8*E*,*F*). Most mesofrontal DA cells were of medium to large size (~15–30 μm). The proximal dendritic arbor was often visible with fast blue labeling, and although the orientation of these processes varied, many PBPG, A9*d* and A8 cells had mediolateral oriented dendrites.

Dorsolateral Granular Frontal Cortex (Prefrontal)

A striking feature of the distribution of DA cells projecting to the dorsolateral granular frontal cortex (as well as precentral cortical areas, see below) was the relative abundance of these neurons in the lateral portions of the dopaminergic cell groups, notably in A9*d* and A8 RRA (Figs 10, 11 and 16), as compared to the distribution of DA cells innervating the medially situated PL and cingulate areas (Figs 12, 13 and 16).

The vast majority of RL/TH neurons following injections in areas 46, 12vl and 8B were observed in the dorsal aspects of A8–A10 and at levels of and caudal to, the red nucleus and the rootlets of the third cranial nerve. The few RL/TH cells observed rostral to the red nucleus were scattered primarily in the parabrachial pigmented nucleus (PBPG) of the VMT and in the region dorsal to the SNpc, i.e. A9 dorsalis (A9*d*). At the level of the rootlets of the third cranial nerve, RL/TH cells were observed primarily in the dorsolateral PBPG and in the A9*d* (Figs 10*C* and 11*C*). Few RL/TH cells were located ventrally to A9*d* in the SNpc, with the exception of DY/TH cells innervating area 12vl. RL/TH cells were observed throughout the full medial-lateral extent of the A9*d* region (Fig. 10*D*). RL/TH cells were not observed in the rostromedial A10 nuclei, i.e. the rostral linear, interfascicular or paranigral nuclei. At the level of the interpeduncular nucleus (IP), a similar distribution pattern of RL/TH cells was observed, with many mesofrontal cells located in the lateral PBPG just ventral to the red nucleus and in the laterally contiguous A9*d* (Figs 10*D* and 11*D*). Again, only occasionally were double-labeled cells present in the rostral linear, interfascicular nuclei or PN at this level.

The greatest number of RL/TH cells was observed at the level of the decussation of the superior cerebellar peduncle. These cells were distributed primarily in the caudal PBPG, A9*d* and the A8 RRA. Many neurons were located in the dorsal A8 region medial to, and within the fibers of the medial lemniscus [Figs 10*E*, 11*E* and 16*C*,*D* (circles)]. Fewer cells were located lateral to the medial lemniscus in the lateral SNpc region. Occasionally, RL/TH cells were observed along the midline in the central linear A10 nucleus. In more caudal sections, a large population of RL/TH neurons was observed in the dorsal aspect of the A8 RRA [Figs 10*F*,*G*, 11*F*,*G*, 16*E* (circles)]. Very few neurons were observed in the ventral portion of the A8 region. In caudal sections at the level of the trochlear nucleus and medial longitudinal fasciculus, RL/TH cells were observed in a region continuous with A8 and merging caudally with the laterally displaced noradrenergic cells of the locus coeruleus (Fig. 10*G*). Numerous RL/TH, presumably noradrenergic cells were observed in the locus coeruleus, bilaterally (Figs 10*H* and 16*F*).

Only a few scattered RL/TH cells were observed in the ventral mesencephalon contralateral to the cortical injection. These neurons were localized in the same dopaminergic regions as the ipsilateral cells. No RL/TH neurons were observed in the anterior diencephalic A12 and A13 dopaminergic cell groups although RL non-immunoreactive neurons were present in these regions. Several RL neurons were observed in the peri- aqueductal gray

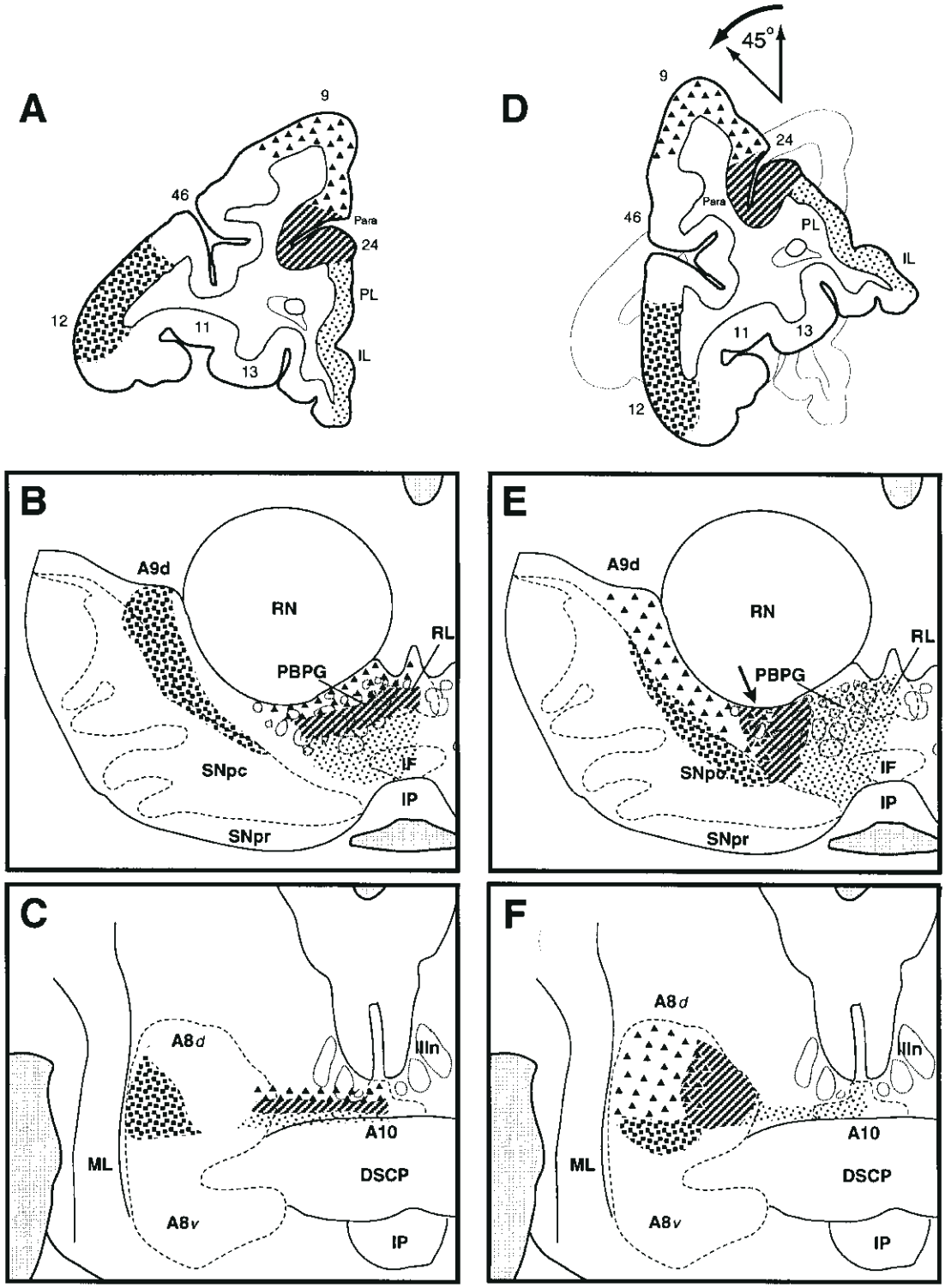

Figure 18. Hypothetical scheme of the topographic organization of midbrain dopamine cells innervating the frontal areas injected in this study (although not shown, this model also includes the precentral areas as well). (*A*) The patterned/shaded areas represent the prefrontal regions injected in the present study, but do not necessarily reflect cytoarchitectonic boundaries. (*B*,*C*) The patterns and shades delineate regions of the ventral mesencephalon *predicted* to innervate the prefrontal areas in (*A*) of the same pattern or shade, if these projections are topographically ordered in the ML and DV dimensions. Thus, the medial areas (PL, area 24 and 9/8B) would be predicted to be innervated by the medial PBPG and linear nuclei of the VMT, whereas the more lateral areas (46 and 12) would be expected to be more significantly innervated by the lateral DA groups, A9*d* and the retrorubral area. Similarly, a crude dorsoventral topography might be anticipated in which the DA cells innervating area 9/8B would be located dorsally to those innervating the anterior cingulate and prelimbic cortex. (*D*) As a simple topographic relationship is not readily apparent in the macaque mesofrontal system, we propose an oblique topographic model. As described in the text, a 45° rotation of the forebrain or midbrain section results in an arrangement of these prefrontal regions that topographically matches (primarily in the ML dimension) the *actual* distribution (*E*,*F*) of DA cells innervating these areas. (*E*,*F*) Schematic representation of the midbrain regions innervating prefrontal areas. This figure is clearly simplified, emphasizing the region from which the prefrontal area receives its most dense input. Thus, the medially located PL and IL areas receive dense projections from the medial PBPG and CL, whereas the more lateral areas 9 and 46 are heavily targeted by the lateral DA cells in A9*d* and A8. See text for details.

(Aaq) and a few of these cells were TH immunoreactive (see Fig. 11*D*).

The general distribution of mesencephalic dopaminergic neurons is very similar for all dorsolateral granular frontal areas injected [areas 46 (including part of area 9d), 12vl and 8B]; however, some specific differences were observed for these areas. Case 0921 contained a diamidino yellow injection into the ventrolateral portion of the prefrontal cortex, area 12, in addition to the fast blue area 46 injection. Although the fast blue injections were far superior in labeling ventral mesencephalic neurons, many DY cells were observed in the midbrain. The general distribution of the RL/TH cells was similar in this case; however, RL/TH cells were noted in more ventral aspects of A9 and A10 (Fig. 11*D*,*E*). Some RL neurons, not exhibiting TH immunoreactivity, particularly in the region of the lateral mammillary nucleus, contained both DY and FB fluorochromes, indicating axonal collateralization to area 46 and area 12. Only one TH-immunoreactive cell containing both retrograde fluorochromes was observed (star in Fig. 11*E*). RL/TH neurons innervating area 8B and area 46 were similar, although area 8B DA cells were somewhat more abundant in the more medial aspects of A9*d* and PBPG. However, as the injection in case 1218 (area 8B) was relatively small, fewer RL neurons were observed in the ventral midbrain, thus limiting our analysis.

Medial Frontal Cortex

The injection centered in the PL (case 1004) yielded RL/TH cells in the dorsal PBPG (Fig. 12*C*,*D*), A9*d* (Fig. 12*B*,*D*) and A8 (Fig. 12E–G). In contrast to the dorsolateral cortex, however, considerably more RL/TH neurons were observed in the A10 midline nuclei of the VMT (RLi and CLi) in case 1004, than following injections into the dorsolateral granular frontal or precentral injections (Fig. 12*C-G*). Particularly prominent were PL-projecting DA cells in the CLi of more caudal midbrain sections (Fig. 12*F*). Conversely, fewer PL DA neurons were observed in the lateral PBPG, A9*d* and A8 regions as compared to the dorsal frontal areas (compare Figs 12*D* to 10*D* and 15*D*; 12*F* to 10*F* and 15*F*; see also Fig. 16).

The fast blue injection into the PL and IL (Fig. 16) yielded a similar distribution of RL/TH neurons concentrated in the A10 midline nuclei of the VMT (RLi and CLi) and PBPG [Fig. 16*B–E* (triangles)]. Similar to case 1004, fewer RL/TH neurons were observed in the lateral PBPG, A9*d* and A8. See below for a more detailed comparison of the distribution of RL/TH cells innervating area 46 with those innervating PL/IL in this case.

The anterior cingulate injection yielded a distribution of RL/TH cells located between the more medially concentrated neurons innervating the PL area and the more laterally concentrated dorsal frontal-projecting neurons (Fig. 13). Thus, fewer RL/TH neurons were observed in the VMT midline nuclei as compared to the PL injection (compare Fig. 13*C* to 12*C* and 13*E–G* to 12*E–G*; also see Fig. 16*D–F*). Unlike the PL, the cingulate cortex appears to be more significantly innervated by A8 and A9*d* DA cells, as are the dorsolateral and precentral frontal areas. Nevertheless, DA cells innervating the cingulate were typically located somewhat more medially than those innervating the dorsolateral and precentral DA cortices (compare Figs 13*D* to 10*D* and 13*G* to 10*F*; also see Fig. 17).

Precentral Cortex

Cases with injections in area 6M (also including the granular frontal area 8B) (case 0728) and in dorsomedial area 4 (case 0123) yielded a distribution of RL/TH neurons very similar to those innervating the dorsolateral granular frontal cortical areas. Again, the majority of RL/TH cells innervating the dorsomedial precentral cortical areas were observed in the dorsolateral PBPG, A9*d* and the dorsal A8 region (Figs 14 and 15). Few RL/TH cells were distributed in the midline VMT nuclei (RLi and CLi), PN, the SNpc and ventral A8. It is our impression that more RL/TH cells innervating these cortical areas, as compared to the more rostral dorsal prefrontal areas, are located in more caudal aspects of the midbrain, particularly in the RRA, than in the more rostral region of the red nucleus. This was especially evident for the injections in the primary motor cortex (compare Figs 10*F* and 15*F*), suggesting a rough rostro-caudal topography.

Comparison of the Distributions of Dorsal Frontal- and Ventromedial-projecting DA Neurons

To obtain a precise comparison of the distribution of DA cells innervating topographically distinct frontal cortical regions we injected two fluorochromes into dorsal and ventromedial areas of the same animal [case 0408 (Figs 7*B*, 16 and 17*J–L*)]. To strengthen the conclusions from this single case, we also compared the distribution of RL/TH cells from dorsal and ventromedial frontal injections made in separate cases by plotting the labeled cells on the same midbrain sections (representative rostral and caudal sections) (Fig. 17*A–I*). Both of these methods uncovered a coarse-grained mediolateral topography in the distribution of dopaminergic frontal cortical-projecting neurons (Fig. 17*A–C*) in which distinct, although partially overlapping, populations of dopamine neurons innervate these different cortical regions (Fig. 17*D–F*). This topography is particularly evident if one compares the distribution of DA neurons innervating the dlPFC with that of the medial prefrontal (PL)-projecting neurons (Fig. 17*G–I*). This topographic relationship was confirmed directly in case 0408 (Fig. 17*J–L*). In rostral sections, the PBPG represents a region of significant overlap of these two populations (Fig. 17*H*). Such overlap is less evident in the caudal midbrain (Fig. 17*I*,*L*), in which the mPFC-projecting DA neurons are concentrated in CLi and dlPFC neurons are more abundant in the RRA.

In addition to the elucidation of topography in the mesofrontal DA system, cases presently reported in which two flurochromes were injected in different areas of the same animal (case 0921 and 0408) allowed us to examine directly the extent of axonal collateralization of DA cortically projecting cells. In both of these cases, RL mesencephalic neurons infrequently contained both retrograde fluorochromes (Figs 11 and 16). This was particularly the case for RL/TH neurons. In case 0408, a few TH-immunoreactive neurons in the midbrain contained both fast blue and fluororuby, indicating projections to both ventromedial and dorsolateral frontal cortex (Fig. 16*C*,*D*). Interestingly, significantly more neurons containing both retrograde flurochromes and TH-immunoreactivity were evident in the locus coeruleus (Fig. 16*F*).

Non-dopaminergic Retrogradely-labeled Mesencephalic Neurons

Injections in all frontal cortical areas examined yielded numerous RL/TH immunonegative, presumably non-dopaminergic neurons in the ventral mesencephalon. These cells were distributed primarily in the rostromedial ventral mesencephalic tegmentum (Figs 10*A*,*B*, 11*A*,*B* and 12*A*,*B*); however, RL non-TH neurons were observed in all regions of the ventral mesencephalon. The rostral-most of these non-dopaminergic cells may represent cells of the supramammillary region and

lateral hypothalamic nucleus. The non-dopaminergic neurons present in the A8–A10 cell groups possessed no obvious morphological characteristics that could be easily distinguished from RL/TH cells. Interestingly, the PL injection produced the greatest number of non-TH RL neurons in the caudal mammillary region/rostromedial VMT (Fig. 12*A*,*B*). The second largest number of non-TH cells in this region was observed following injections in area 46 (Fig. 10*A*,*B*). The anterior cingulate injection yielded considerably fewer cells (Fig. 13*A*) and even fewer RL neurons were observed in the rostral VMT following precentral injections (Figs 14*A*,*B* and 15*A*,*B*). In the present study we did not attempt to identify the neurotransmitter content of these neurons.

Discussion

This study represents a comprehensive examination of the brainstem distribution of histochemically identified DA neurons which project to the macaque frontal cortex. The results of the present study represent a departure from the traditional view that mesocortical DA afferents arise from the VTA exclusively, in that DA afferents to the frontal lobe, as a whole, arise from the dorsal regions of all three dopamine cell groups, A8–A10, and are governed by a broad mediolateral topography. Thus, the proportion of A8–A10 neurons projecting to the cerebral cortex depends on the region innervated, suggesting that the mesofrontal DA system is not a unitary afferent system, but may be comprised of multiple, potentially functionally distinct projections. This study also revealed that the non-DA population of frontal cortex-projecting neurons represents a considerable proportion of the mesencephalic innervation of the frontal cortex, illustrating the potential neurochemical diversity of midbrain influences on frontal lobe operations.

Topographic Organization of the Mesofrontal DA System

Two aspects of the organization of the mesofrontal projections were particularly salient: (i) The midbrain origin of DA inputs to the frontal lobe is widespread. That is, all frontal cortical areas injected revealed RL DA neurons in the dorsal aspect of A8–A10. (ii) The proportion of RL cells within these DA cell loci varied significantly between the various frontal cortical areas. Although DA neurons innervating area 46 are primarily located laterally to those projecting to prelimibic areas, certain anomalies to a simple topographic scheme were observed (Figs 17 and 18). Thus, DA cells innervating areas 9/8B (and 6M) do not lie medial to those innervating area 46 as would be expected. Further, many area 24-projecting DA cells do not lie medial to those projecting to more lateral located cortical areas, and finally, cells innervating lateral prefrontal area 12 are not located lateral to area 46-projecting cells, but instead are observed ventral to these neurons.

However, we discovered that if one simply rotates the frontal coronal section ~45° along the vertical axis of the midline (e.g. counterclockwise for a left hemisphere section; clockwise for the right hemisphere) (Fig. 18), a topographic relationship emerges such that areas 9/8B, 46 and 12 are in approximately the same mediolateral plane, and reveals their innervation from DA cells located in similar mediolateral positions, i.e. the more lateral PBPG, A9*d* and A8. Moreover, in this arrangement, the PL is medial to area 24, consistent with the distribution of DA cells innervating these regions, and the DA neurons innervating both area 24 and PL being located medial to area 9/8B-projecting cells, again, consistent with the rotated cortex. This model predicts that the orbital areas 11 and 13 receive the majority of their DA input from midline midbrain DA neurons, exhibiting a pattern similar to the PL innervation. Furthermore, the infralimbic cortex would be expected to be innervated by the most medial DA cells, predominantly located in the midline VMT linear nuclei, consistent with the present observations. The presently described mediolateral topography is indeed coarse, reflecting only the majority of DA inputs to a given area, but is consistent with previous findings (Porrino and Goldman- Rakic,1982; Gaspar *et al.*, 1992).

Although mesofrontal afferents arise exclusively from the dorsal tier of midbrain DA neurons, as observed by others (Porrino and Goldman-Rakic,1982; Lewis *et al.*, 1988; Gaspar *et al.*, 1992, Oeth and Lewis, 1992) evidence for a dorsoventral ordering within this compartment is less apparent in our material. Nevertheless, DA neurons innervating area 12 were observed ventral to most other cortically projecting cells, suggesting a weak dorsoventral relationship (Fig. 17*E*,*F*). Most of our injections of the frontal lobe were in roughly equivalent anterior–posterior planes, with the exception of the supplementary motor and primary motor cortex injections, so examination of topography in this domain was not as clear. Nevertheless, DA neurons innervating the precentral cortex, although distributed in a pattern very similar to those innervating other dorsal frontal areas (areas 46 and 8), appear to extend further caudally in the RRA than DA neurons projecting to other frontal areas examined, suggestive of a crude rostral-caudal topography.

Parallel Mesofrontal DA Projections

As discussed above, the dorsal areas, including area 4, are heavily innervated by lateral PBPG, A9*d* and A8 neurons. In contrast, the ventromedial cortical-projecting DA neurons are located in the medial PBPG, linear VMT nuclei and medial A8. It is tempting to speculate that these differing DA cell distributions represent distinct parallel dopaminergic inputs to the dorsal and ventromedial frontal cortex. Deutch *et al.* (1993) have provided evidence for distinct mesoprefrontal DA systems in the rodent, possessing unique cellular origins, as well as differing biochemical profiles. A wealth of data in the rodent demonstrates the heterogeneous distribution of neurochemicals and afferent inputs in the ventral mesencephalon (Oades and Halliday, 1987; Gerfen, 1992), suggesting that the functionally unique properties of the mesoprefrontal DA systems are due, in part at least, to the different midbrain populations of DA cells, as opposed to differential presynaptic regulation in the PFC (Deutch *et al.*, 1993).

At present, little is known about the chemical and hodological organization of the primate mesencephalon. Evidence for the differential distribution of neurochemically characterized afferents in the midbrain that precisely matches the distribution of DA cells of the dorsal or ventromedial mesofrontal 'pathways' is lacking in primates. However, several studies have demonstrated that the dorsal portions of the A8–A10 cell groups, i.e. the location of mesofrontal neurons as a whole, may represent a distinct chemoanatomic compartment of the dopaminergic mesencephalon (Gerfen *et al.*, 1985, 1987; Gaspar *et al.*, 1992, 1993; McRitchie *et al.* 1996). For example, Gaspar *et al.* (1992) have demonstrated that the calcium-binding protein calbindin D_{28k} (CB) is colocalized in a subpopulation of midbrain TH neurons which shares the same topographic location as mesofrontal DA cells. At least some of these CB/TH cells do indeed, project to the frontal cortex (Gaspar *et al.*, 1993; S.M. Williams and P.S. Goldman-Rakic, unpublished observations).

The presence of calbindin in this subset of DA neurons may be related to the electrophysiological properties of these neurons, and has been related to the higher resistance of CB-containing midbrain dopamine neurons to the neurodegeneration observed in Parkinson's disease and animal models of this illness (Gerfen *et al.*, 1987; Manaye *et al.*, 1991; Yamada *et al.*, 1991; Parent and Lavoie, 1993). Furthermore, the distribution of the dopamine D2 receptor (Meader-Woodruff *et al.*, 1994; Haber *et al.*, 1995a,b) and the dopamine transporter (Haber *et al.*, 1995a,b) appear to be more prevalent in the ventral tier of midbrain DA neurons, i.e. SNpc and ventral A8, and thus less associated with the mesocortical compartment. Similarly, the varied distribution of excitatory amino acid-containing, GABAergic, peptidergic and monoaminergic midbrain afferents suggests that the activity of mesotelencephalic DA neurons may be regulated differentially by a host of inputs (Oades and Halliday, 1987; Seutin *et al.*, 1993). Of particular interest will be the elucidation of the precise midbrain distribution of these afferents in relation to the topographic organization of the mesofrontal DA projections.

Species Differences: Is the Retrorubral-frontal Cortex Projection a Primate Specialization?

The present results, as well as those of previous studies (Porrino and Goldman-Rakic, 1982; Lewis *et al.*, 1988; Gaspar *et al.*, 1992; Oeth and Lewis, 1992), demonstrate that the areal and laminar expansion of the dopaminergic innervation of the frontal lobe of monkeys, as compared to rodents, is paralleled by significant expansion and reorganization of the midbrain cellular origin of this projection. Thus, the rodent frontal DA innervation, which is most dense in the prefrontal and anterior cingulate cortices, arises primarily from neurons located in the VTA, with substantially fewer cells located in A9 (medial A9) and virtually no input from the RRA (Deutch *et al.*, 1988). Similarly, the cells of origin of the DA innervation of the neocortex in cats appear to be restricted to the midline VTA nuclei (Scheibner and Tork, 1987). It appears, therefore, as suggested by Gaspar *et al.* (1992), that during primate evolution the dopamine innervation expanded into these more dorsolateral areas of the macaque frontal lobe (e.g. premotor, motor and the phylogenetically newer dorsolateral prefrontal areas), as well as into their superficial layers, and a concomitant lateral shift appears to have occurred in the midbrain cellular origin of these projections. Recently, McRitchie *et al.* (1996) have demonstrated a greater number of A8 neurons in the human mesencephalon as compared to the rodent, relative to the other DA cell groups, suggesting species-specific specialization of the DA cell groups. This relative increase in the size of the A8 cell group may indeed reflect the expansion of the neocortex, as well as the expansion of the neocortical DA afferents in anthropoid primate species.

Of the midbrain DA cell groups, the primate A8 efferents appear to have undergone the most salient reorganization. In the rodent the RRA projects to the majority of mesolimbic structures (e.g. bed nucleus of the stria terminalis, nucleus accumbens, olfactory tubercle and amygdala), mesostriatal structures (especially the ventrolateral caudoputamen) and allocortex (piriform and entorhinal cortices) (reviewed in Bjorklund and Lindvall, 1984). In contrast to our data in the macaque, Deutch *et al.* (1988) did not observe retrorubral projections to neocortical areas in the rat. Although there is evidence that this region projects to the caudate and putamen in primates (Szabo, 1980), it does not appear to project to the nucleus accumbens in this species (Lynd-Balta and Haber, 1994; Williams and Goldman-Rakic, 1998). Thus, in primates the A8 region is intimately associated with the dorsal mesofrontal and dorsal striatal innervation and may not be a major source of mesolimbic dopamine (at least to the ventral striatum) in the primate as it is in rodents.

Although cortically projecting neurons were observed in the RRA in two previous studies of the primate mesofrontal system (Porrino and Goldman-Rakic, 1982; Gaspar *et al.*, 1992), this projection has not been considered robust. Quantitative analysis in the owl monkey revealed that <15% of mesofrontal (motor, SMA and lateral PFC) DA cells were observed in the RRF, with little variability between frontal areas (Gaspar *et al.*, 1992). However, estimates in a few cases in this study suggest that many more DA cells, ~40%, projecting to dorsal frontal areas are located in A8. Although species differences between Old and New World monkeys could be responsible for this discrepancy, definitions of the A8 region may also underlie these differences.

The present results, which are the first to demonstrate the origin of the DA innervation of the medial frontal cortex in primates, are particularly relevant to issues of prefrontal cortical homology between rodents and primates. Based on a review of connectional data, including an analysis of the dopamine innervation, and functional studies, Preuss and Goldman-Rakic (1991) and Preuss (1994) have suggested that rodents lack homologues of the dorsolateral granular frontal (prefrontal) cortex of primates. It is the medial prefrontal areas of the primate (areas PL and IL), according to their model, that the rodent medial frontal cortex resembles. Our data demonstrating a robust midline VMT input to the medial prefrontal cortex (PL), but not to the dlPFC of the macaque, coupled with the predominant midline DA innervation of the rodent PFC support the idea that these medial regions are homologous. Furthermore, these anatomical data would appear to substantiate the claim that the dorsolateral granular frontal cortical areas in primates have no homologues in rodents (Preuss, 1994).

Functional and Clinical Implications

The widespread distribution and topographic organization of frontal cortex-projecting DA neurons may influence our understanding of the role of the mesocortical DA system in schizophrenia and Parkinson's disease. Our views regarding the function of dopamine in the frontal cortex of primates, including humans, has been predicated on the assumption that this afferent system arises from the VTA, as it does in the rodent. The present demonstration that the dorsal and ventromedial frontal cortices are innervated by relatively distinct populations of mesencephalic DA cells, with the dorsal regions heavily targeted by DA cells which reside outside of the VTA, may suggest that these projections are functionally dissociable. Behavioral studies of these different prefrontal cortical domains in primates suggests that the dorsal PFC regions are intimately involved in spatial and object working memory functions (Fuster, 1985; Goldman-Rakic, 1987), as well as in the control of eye movements (Bruce and Goldberg, 1984), whereas the ventromedial cortices have been less associated with spatial processes and more so with emotional and autonomic functions, response inhibition and stimulus significance (Fuster, 1984; see also discussion in Yeterian and Pandya, 1991). The dorsal precentral cortices are, of course, critical for the planning and execution of voluntary movement. It is tempting to speculate that the DA innervations of the dorsal and ventromedial frontal regions possess unique functional characteristics due to different cellular origins and afferent inputs in the midbrain, and

that these DA projections contribute to the overall functional specialization of the frontal cortex.

Models of DA dysfunction in schizophrenia and of the action of antipsychotic drugs are largely based upon a hodological scheme which fails to recognize the significant, and potentially functionally distinct, non-VTA frontal cortical DA inputs in the primate, particularly to the dorsal cortical areas. As the dlPFC is one of only a few specific cortical areas that has been repeatedly implicated in the pathophysiology of schizophrenia (Levin, 1984**;** Weinberger *et al.*, 1986, 1988; Goldman-Rakic, 1991), particularly in regard to cognitive deficits, the present results demonstrate a need to examine further the A9 and A8 neurons, in addition to the A10 DA cells, that give rise to this projection. Furthermore, as the dorsolateral PFC DA innervation has been repeatedly associated with spatial working memory processes, and as schizophrenic patients have demonstrated deficits on such cognitive tasks (Park and Holzman, 1992), the A8 and A9*d*, in addition to the A10, neurons subserving this DA innervation appear to be good targets for novel drugs to combat such deficit symptoms.

Degeneration of the mesocortical DA system is well established in Parkinson's disease (Price *et al.*, 1978; Scatton *et al.*, 1983; Gaspar *et al.*, 1991), although the areas involved and the extent of degeneration is not clear. Interestingly, Deutch *et al.* (1986) have demonstrated that in MPTP-treated monkeys, lateral A8 neurons appear to be the most sensitive to neurotoxicity. Given the significant innervation of the motor, premotor and dorsal prefrontal areas by lateral A8 neurons, the loss of such cells in experimental animal models of PD, and potentially in PD, may contribute to the extrapyramidal and cognitive deficits observed in these subjects. Thus, the widespread distribution of mesofrontal DA cells and the suggestion of parallel, unique projections may, in part, underlie the heterogeneity of cognitive and affective symptoms in both Parkinson's disease and schizophrenia.

Notes

Address correspondence to Patricia Goldman-Rakic, Section of Neurobiology, Yale University School of Medicine, 333 Cedar Street, SHM, New Haven, CT 06510, USA.

References

Akbarian S, Bunney WE Jr, Potkin SG, Wigal SB, Hagman JO, Sandman CA, Jones EG (1993) Altered distribution of nicotinamide-adenine dinucleotide phosphate-diaphorase cells in frontal lobe of schizophrenics implies disturbances of cortical development. Arch Gen Psychiat 50:169–177.

Arsenault M-Y, Parent A, Seguela P, Descarries L (1988) Distribution and morphological characteristics of dopamine-immunoreactive neurons in the midbrain of the squirrel monkey (*Saimiri sciureus*). J Comp Neurol 267:489–506.

Benes FM, McSparren J, Bird ED, SanGiovanni JP, Vincent SL (1991) Deficits in small interneurons in prefrontal and cingulate cortices of schizophrenic and schizoaffective patients. Arch Gen Psychiat 48: 996–1001.

Berger B, Trottier S, Gaspar P, Verney C, Alvarez C (1986) Major dopamine innervation of the cortical motor areas in the cynomolgous monkey. A radioautographic study with comparative assessment of serotonergic afferents. Neurosci Lett 72:121–127.

Berger B, Gaspar P, Trottier S (1988a) Catecholaminergic innervation of the human cerebral cortex: a phylogenetic perspective. Progr Catecholamine Res

Berger B, Trottier S, Verney C, Gaspar P, Alvarez C (1988b) Regional and laminar distribution of the dopamine and serotonin innervation in the macaque cerebral cortex: a radioautographic study. J Comp Neurol 273:99–119.

Berger B, Verney C, Goldman-Rakic PS (1991) In: Neurodevelopment, aging and cognition (Kostovic I, Knezevic S, Spilich G, eds). Birkhauser.

Berman AL (1968) The brainstem of the cat. A cytoarchitectonic atlas with stereotaxic coordinates. Madison: University of Wisconsin Press.

Bjorklund A, Lindvall O (1984) Dopamine-containing systems in the CNS. Handbook Chem Neuroanat 2:55–121.

Brozoski TJ, Brown RM, Rosvold HE, Goldman PS (1979) Cognitive deficit caused by regional depletion of dopamine in prefrontal cortex of rhesus monkey. Science 205:929–932.

Bruce CJ, Goldberg ME (1984) Physiology of the frontal eye fields. Trends Neurosci 7:436–441.

Dahlstrom A, Fuxe K (1964) Evidence for the existence of monoamine containing neurons in the central nervous system. I. Demonstration of monoamines in the cell bodies of brain stem neurons. Acta Physiol Scand 62(Suppl. 232):1–55.

Deutch AY, Elsworth JD, Goldstein M, Fuxe K, Redmond DE, Sladek JR, Roth RH (1986) Preferential vulnerability of A8 dopamine neurons in the primate to the neurotoxin 1-methyl-4-phenyl-1,2,3,6-tetrahydropyridine. Neurosci Lett 68:51–56.

Deutch AY, Goldstein M, Baldino F Jr, RH Roth (1988) The telencephalic projections of the A8 dopamine cell group. Ann NY Acad Sci 537:27–50.

Deutch AY, Bean AJ, Bissette G, Nemeroff CB, Robbins RJ, Roth RH (1987) Stress-induced alterations in neurotensis, somatostatin and corticotropin-releasing factor in mesotelencephalic dopamine system regions. Brain Res 417:350–354.

Deutch AY, Lee MC, Gillham MH, Cameron D, Goldstein M, Iadorola MJ (1991) Stress selectively increases Fos protein in dopamine neurons innervating the prefrontal cortex. Cereb Cortex 1:273–292.

Deutch AY, Bourdelais AJ, Zahm DS (1993) The nucleus accumbens core and shell: accumbal compartments and their functional attributes. In: Limbic motor circuits and neuropsychiatry (Kalivas PW, Barnes CD, eds), pp. 45–77. Boca Raton, FL: CRC Press.

Felten DL, Sladek JR Jr (1983) Monoamine distribution in primate brain V. monoaminergic nuclei: anatomy, pathways and local organization. Brain Res Bull 10:171–284.

Francois C, Percheron G, Yelnik J, Heyner S (1985) A histological atlas of the macaque (*Macaca mulatta*) substantia nigra in ventricular coordinates. Brain Res Bull 14:349–367.

Fuster JM (1984) Behavioral electrophysiology of the prefrontal cortex. Trends Neurosci 7:408–414.

Fuster JM (1985) The prefrontal cortex and temporal integration. In: Cerebral cortex (Jones EG, Peters A, eds), pp. 151–177. New York: Plenum.

Gallyas F (1979) Silver staining for myelin by means of physical development. Neurol Res 1:203–209.

Gaspar P, Berger B, Febvret A, Vigny A, Henry JP (1989) Catecholamine innervation of the human cerebral cortex as revealed by comparative immunohistochemistry of tyrosine hydroxylase and dopamine-beta-hydroxylase. J Comp Neurol 279:249–271.

Gaspar P, Duyckaerts C, Alvarez C, Javoy-Agid F, Berger B (1991) Alterations of dopaminergic and noradrenergic innervations in motor cortex in parkinson's disease. Ann Neurol 30:365–374.

Gaspar P, Heizmann CW and JH Kaas (1993) Calbindin D-28K in the dopaminergic mesocortical projection of a monkey (*Aotus trivirgatus*). Brain Res 603:166–172.

Gaspar P, Stepniewska I, JH Kaas (1992) Topography and collateralization of dopaminergic projections to motor and lateral prefrontal cortex in owl monkeys. J Comp Neurol 325:1–21.

Gerfen CR (1992) The neostriatal mosaic: multiple levels of compartmental organization. J Neural Transm 36:43–59.

Gerfen CR, Baimbridge KG, Miller JJ (1985) The neostriatal mosaic: compartmental distribution of calcium binding protein and parvalbumin in the basal ganglia of rat and monkey. Proc Natl Acad Sci USA 82:8780–8784.

Gerfen CR, Baimbridge KG, Thibault J (1987) The neostriatal mosaic: biochemical and developmental dissociation of patch-matrix nigrostriatal systems. J Neurosci 7:3935–3944.

Glantz LA, Lewis DA (1993) Synaptophysin immunoreactivity is selectively decreased in the prefrontal cortex of schizophrenic subjects. Soc Neurosci Abstr 19:201.

Goldman-Rakic PS (1987) Circuitry of the prefrontal cortex and the regulation of behavior by representational knowledge. In: Handbook of physiology, Vol. 5 (Plum F, Mountcastle V, eds), pp. 373–417. Bethesda, MD: American Physiological Society.

Goldman-Rakic PS (1991) Prefrontal cortical dysfunction in schizophrenia: the relevance of working memory. In: Psychopathology and the brain (Carroll BJ, Barret JE, eds), pp. 1–23. New York: Raven Press.

Haber SN, Kunishio K, Mizobuchi M, Lynd-Balta E (1995a) The orbital and medial prefrontal circuit through the primate basal ganglia. J Neurosci 15:4851–4867.

Haber SN, Ryoo H, Cox C, Lu W (1995b) Subsets of midbrain dopaminergic neurons in monkeys are distinguished by different levels of mRNA for the dopamine transporter: comparison with the mRNA for the D_2 receptor, tyrosine hydroxylase and calbindin immunoreactivity. J Comp Neurol 362:400–410.

Halliday GM, Tork I (1986) Comparative anatomy of the ventromedial mesencephalic tegmentum in the rat, cat, monkey and human. J Comp Neurol 252:423–445.

Kishka U, Kammer T, Maier S, Weisbrod M, Thimm M, Spitzer M (1996) Dopaminergic modulation of semantic network activation. Neuropsychologia 34:1107–1113.

Levin S (1984) Frontal lobe dysfunctions in schizophrenia, II: impairments of psychological and brain functions. J Psychiat Res 18:27–55.

Levitt P, Rakic P, Goldman-Rakic PS (1984) Comparative assessment of monoamine afferents in mammalian cerebral cortex. In: Monoamine innervation of cerebral cortex, pp. 41–59. New York: Alan R. Liss

Lewis DA, Campbell MJ, Foote SL, Goldstein M, Morrison JH (1987) The distribution of tyrosine-hydroxylase-immunoreactive fibers in primate neocortex is widespread but regionally specific. J Neurosci 7:279–290.

Lewis DA, Foote S L, Goldstein M, Morrison JH (1988) The dopaminergic innervation of the monkey prefrontal cortex: a tyrosine hydroxylase immunohistochemical study. Brain Res 449:225–243.

Lynd-Balta E, Haber SN (1994a) The organization of midbrain projections to the ventral striatum in the primate. Neuroscience 59:609–623.

Luciana M, Depue RA, Arbisi P and Leon A (1992) Facilitation of working memory in humans by a D2 dopamine receptor agonist. J Cogn Neurosci 4:58–68.

Luciana M, Collins PF (1997) Dopaminergic modulation of working memory for spatial but not object cues in normal humans. J Cogn Neuroci.

Manaye KF, Sonsella PK, Brooks BA, German DC (1991) Calbindin-D28K is located in midbrain dopaminergic neurons which are resistant to MPTP-induced degeneration. Soc Neurosci Abstr 17:1275.

McRitchie DA, Hardman CD, Gallida GM (1996) Cytoarchitectural distribution of calcium binding proteins in midbrain dopaminergic regions of rats and humans. J Comp Neurol 364:121–150.

Meader-Woodruff JH, Damask SP, Watson SJ Jr (1994) Differential expression of autoreceptors in the ascending dopamine systems of the human brain. Proc Natl Acad Sci USA 91:8297–8301.

Murphy BL, Arnsten AFT, Goldman-Rakic PS, Roth RH (1996a) Increased dopamine turnover in the prefrontal cortex impairs spatial working memory performance in rats and monkeys. Proc Natl Acad Sci USA 93:1325–1329.

Murphy BL, Arnsten AFT, Jentsch JD, Roth RH (1996b) (+)HA966 and clonidine block FG7142-induced increase in prefrontal cortical dopamine turnover and prevent stress-induced spatial workng memory deficits in rats and monkeys. .

Oades RD, Halliday GM (1987) Ventral tegmental (A10) system: neurobiology. 1. Anatomy and connectivity. Brain Res Rev 12:117–165.

Oeth KM, Lewis DA (1992) Cholecystokinin- and dopamine-containing mesencephalic neurons provide distinct projections to monkey prefrontal cortex. Neurosci Lett 145:87–92.

Olszewski J, Baxter D (1982) Cytoarchitecture of the human brain stem, 2nd edn. New York.

Parent A, Lavoie B (1993) The heterogeneity of the mesostriatal dopaminergic system as revealed in normal and parkinsonian monkeys. Adv Neurol 60:25–33.

Park S, Holzman PS (1992) Schizophrenics show spatial working memory deficits. Arch Gen Psychiat 49:975–982.

Pettegrew JW, Keshavan MS, Panchalingam K, Strychor S, Kaplan DB, Tretta MG, Allen, M (1991) Alterations in brain high-energy phosphate and membrane phospholipid metabolism in first-episode, drug-naive schizophrenics: a pilot study of the dorsal prefrontal cortex by *in vivo* phosphorus 31 nuclear magnetic resonance spectroscopy. Arch Gen Psychiat 48:563–568.

Poirier LJ, Giguere M, Marchand R (1983) Comparative morphology of the substantia nigra and ventral tegmental area in the monkey, cat and rat. Brain Res Bull 11:371–397.

Porrino L J, Goldman-Rakic PS (1982) Brainstem innervation of prefrontal and anterior cingulate cortex in the rhesus monkey revealed by retrograde transport of HRP. J Comp Neurol 205:63–76.

Preuss TM, Goldman-Rakic PS (1991) Architectonics of the parietal and temporal association cortex in the strepsirhine primate *galago* compared to the anthropoid primate *macaca*. J Comp Neurol 310:475–506.

Preuss T M (1995) Do rats have prefrontal cortex? The Rose–Woolsey–Akert program reconsidered. J Cogn Neurosci 7:1–24.

Price KS, Farley IJ, Hornykiewicz O (1978) Neurochemistry of Parkinson's disease: relation between striatal and limbic dopamine. Adv Biochem Psychopharmacol 19:293–300.

Rioch DM (1948) Studies on the diencephalon of carnivora. Part II. Certain nuclear configurations and fiber connections of the subthalamus and midbrain fo the dog and cat. J Comp Neurol 49:121–153.

Roth RH, Tam S-Y, Ida Y, Yang J-X, Deutch AY (1988) Stress and the mesocorticolimbic dopamine systems. Ann NY Acad Sci 537:138–147.

Sawaguchi T, Goldman-Rakic PS (1991) D1 dopamine receptors in prefrontal cortex: involvement in working memory. Science 251:947–950.

Scatton B, Javoy-Agid F, Rouquier L, Dubois B, Agid Y (1983) Reduction of cortical dopamine, noradrenaline, serotonin and their metabolites in parkinson's disease. Brain Res 275:321–328.

Scheibner T, Tork I (1987) Ventromedial mesencephalic tegmental (VMT) projections to ten functionally different cortical areas in the cat: topography and quantitative analysis. J Comp Neurol 259:247–265.

Selemon LD, Rajkowska G, Goldman-Rakic PS (1995) Abnormally high neuronal density in the schizophrenic cortex. Arch Gen Psychiat 52:805–818.

Sesack SR, Snyder CL, Lewis DA (1995) Axon terminals immunolabeled for dopamine or tyrosine hydroxylase synapse on GABA-immunoreactive dendrites in rat and monkey cortex. J Comp Neurol 363:264–280.

Seutin V, North RA, Johnson SW (1993) Transmitter regulation of mesencephalic dopamine cells. In: Limbic motor circuits and neuropsychiatry (Kalivas PW, Barnes CD, eds), pp. 89–97. Boca Raton, FL: CRC Press.

Smiley JF, Goldman-Rakic PS (1993) Heterogeneous targets of dopamine synapses in monkey prefrontal cortex demonstrated by serial section electron microscopy; a laminar analysis using the silver enhanced diaminobenzidine sulfide (SEDS) immunolabeling technique. Cereb Cortex 3:223–238.

Smiley JF, Levey AI, Ciliax BJ, Goldman-Rakic PS (1994) D_1 dopamine receptor immunoreactivity in human and monkey cerebral cortex: predominant and extrasynaptic localization in dendritic spines. Proc Natl Acad Sci USA 91:1–5.

Szabo J (1980) Organization of ascending striatal afferents in monkeys. J Comp Neurol 189:307–321.

Walker AE (1940) A cytoarchitectural study of the prefrontal area of the macaque monkey. J Comp Neurol 73:59–86.

Weinberger DR, Berman KF, Zec RF (1986) Physiological dysfunction of dorsolateral prefrontal cortex in schizophrenia, I: regional cerebral blood flow (rCBF) evidence. Arch Gen Psychiat 43:114–124.

Weinberger DR, Berman KF, Illowsky BP (1988) Physiological dysfunction of dorsolateral prefrontal cortex in schizophrenia, III: a new cohort and evidence for a monoaminergic mechanism. Arch Gen Psychiat 45:609–615.

Williams GV, Goldman-Rakic PS (1995) Modulation of memory fields by dopamine D1 receptors in prefrontal cortex. Nature 376:572–575.

Williams SM, Goldman-Rakic PS (1993) Characterization of the dopaminergic innervation of the primate frontal cortex using a dopamine-specific antibody. Cereb Cortex 3:199–222.

Yamada T, McGeer PL, Baimbridge K, McGeer EG (1991) Relative sparing in Parkinson's disease of substantia nigra dopamine neurons containing calbindin-D28k. Brain Res 526:303–307.

Yeterian EH, Pandya DN (1991) Prefrontostriatal connections in relation to cortical architectonic organization in rhesus monkeys. J Comp Neurol 312:43–67.